



UNIVERSITAT  
POLITÈCNICA  
DE VALÈNCIA



ESCUELA TÉCNICA  
SUPERIOR INGENIERÍA  
INDUSTRIAL VALENCIA

**INGENIERÍA MECÁNICA Y DE MATERIALES**

**ESTUDIO DE LA CORROSIÓN EN  
MEDIOS CERCANOS A LA SALIVA  
HUMANA DE LAS ALEACIONES BASE  
TITANIO-NIOBIO-PLATA Y TITANIO-  
NIOBIO-COBRE PARA LAS  
APLICACIONES EN CAMPO  
BIOMÉDICO**

**AUTOR: ZAGORSKIY-VIROT, VADIM**

**TUTOR: KLYATSKINA RUSINOVICH, ELIZAVETA**

**Curso Académico : 2020/2021**

# AGRADECIMIENTOS

First of all, I would like to thank Doctor Vicente Amigó Borrás, who was my very first contact during this research internship, who warmly welcomed me to the laboratory where I was able to work.

Then, I also have a special thought for Montse and Mariana, who both helped me in the accomplishment of my research by helping me and by explaining to me the functioning of the different devices present in the laboratory.

Of course, I thank Maria Vinogradova, with whom I worked during this project and with whom I also had long discussions on Russia, France, and on lots of interesting subjects.

I would also like to thank Paco for his explanations, always very rich, detailed and precise on the various results and their meanings.

Finally, thanks to my tutor, Elizaveta Klyatskina, who helped me not only to carry out this work, but also and above all to explain its goals, direction, and expectations. I also remember the time that was given to me on his part, and that of other people who took the time to help me and teach me more.

## RESUMEN

El titanio y sus aleaciones son materiales ampliamente utilizados en el campo biomédico, especialmente en los prótesis dentbucal. De hecho, las propiedades de estas aleaciones de titanio las convierten en los mejores candidatos para las prótesis. Sin embargo, resulta que las cualidades del cobre y de la plata son indispensables en estas aleaciones porque evitan las infecciones y son buenos bactericidas.

Los experimentos realizados en este trabajo ponen en práctica muestras de Ti-35Nb (titanio y 35% de niobio) a las que se añade una cierta cantidad de cobre o plata (2, 4 o 6%).

Estas muestras se obtuvieron previamente mediante las técnicas de metalurgia de polvos que se describirán en este trabajo.

El trabajo se centró en el estudio de la corrosión electroquímica de las muestras. Para ello, mediante un potencióstato, se midieron diferentes variables según el principio del ensamblaje de tres electrodos. A continuación, se analizaron y discutieron los resultados experimentales obtenidos para comprender su significado, su significado, pero también y sobre todo para determinar las razones de las diferencias entre la presencia de cobre y plata en una muestra de base de Ti-35Nb.

**Palabras Clave:** Aleación de titanio, Ti-35Nb, plata, cobre, metalurgia en polvo, corrosión, potenciador, ensamblaje de tres electrodos, implante.

# RESUM

El titani i els seus aliatges són materials àmpliament utilitzats en el camp biomèdic, especialment en els pròtesis dentbucal. De fet, les propietats d'aquests aliatges de titani les converteixen en els millors candidats per a les pròtesis. No obstant això, resulta que les qualitats del coure i de la plata són indispensables en aquests aliatges perquè eviten les infeccions i són bons bactericides.

Els experiments realitzats en aquest treball posen en pràctica mostres de Tu-35Nb (titani i 35% de niobi) a les quals s'afeg una certa quantitat de coure o plata (2, 4 o 6%).

Aquestes mostres es van obtenir prèviament mitjançant les tècniques de metal·lúrgia de pólvores que es descriuran en aquest treball.

El treball es va centrar en l'estudi de la corrosió electroquímica de les mostres. Per a això, mitjançant un potenciostat, es van mesurar diferents variables segons el principi de l'assemblatge de tres elèctrodes. A continuació, es van analitzar i van discutir els resultats experimentals obtinguts per a comprendre el seu significat, el seu significat, però també i sobretot per a determinar les raons de les diferències entre la presència de coure i plata en una mostra de base de Tu-35Nb.

**Paraules Clau:** Aliatge de titani, Tu-35Nb, plata, coure, metal·lúrgia en pols, corrosió, potenciador, assemblatge de tres elèctrodes, implant.

## **ABSTRACT**

Titanium and its alloys are materials widely used in the biomedical field, especially when it comes to the dental prosthesis. Indeed, the properties of these titanium alloys make them the best candidates for prostheses. Nevertheless, it turns out that the qualities of copper and silver are indispensable in these alloys because they prevent infections and are good bactericides.

The experiments carried out corrosion measurement in this work put into practice Ti-35Nb samples (titanium and 35% niobium) to which a certain quantity of copper or silver (2, 4 or 6%) is added.

These samples were previously obtained using powder metallurgical techniques that will be described in this work.

The work focused on the study of the electrochemical corrosion of the samples. For this purpose, using a potentiostat, different variables were measured on the principle of the three-electrode assembly. The experimental results obtained were then analyzed and discussed in order to understand their significance, their meaning, but also and above all to determine the reasons for the differences between the presence of copper and silver in a Ti-35Nb base sample.

**Keywords:** Titanium alloy, Ti-35Nb, silver, copper, powder metalurgy, corrosion, potentiostat, three-electrode assembly, implant.

# INDEX

## DOCUMENTS CONTAINED IN THE TFM :

- DOCUMENT 1: MEMORY.
- DOCUMENT 2: BUDGET.

## CHAPTER 1. MOTIVATION AND OBJECTIVES.....13

1.1. MOTIVATION.....13

1.2. OBJECTIVES.....13

## CHAPTER 2. INTRODUCTION.....14

<b>2.1. HISTORY OF TITANIUM.....</b>	<b>14</b>
2.1.1 TWO FORMS OF TITANIUM.....	15
<b>2.2. WHAT THE CORROSION IS? .....</b>	<b>15</b>
<b>2.3. THE DIFFERENT TYPES OF CORROSION.....</b>	<b>16</b>
2.3.1 NON-AQUEOUS (DRY) CORROSION.....	16
2.3.2 AQUEOUS CORROSION.....	16
2.3.2.1 UNIFORM CORROSION.....	16
2.3.2.2 GALVANIC CORROSION.....	16
2.3.2.3 PITTING CORROSION.....	16
2.3.2.4 INTERGRANULAR CORROSION.....	17
2.3.2.5 CORROSION UNDER STRESS OR STRAIN.....	17
2.3.2.6 BACTERIAL CORROSION.....	17
2.3.2.7 CORROSION BY EROSION AND CAVITATION.....	17
2.3.2.8 STRAY CURRENT CORROSION.....	17
2.3.2.9 SELECTIVE CORROSION (DEALLOYING) .....	17
2.3.2.10 CAVERNOUS CORROSION.....	18

## **CHAPTER 3. MATERIALS AND METHODS.....19**

<b>3.1 MANUFACTURE OF SAMPLES FROM POWDERS.....</b>	<b>19</b>
3.1.1 POWDERS.....	19
3.1.2 MIXING AND HOMOGENIZATION.....	19
3.1.3 FORMING OF POWDERS.....	19
3.1.4 SINTERING.....	20
<b>3.2 SOME PROPERTIES OF WORKING SAMPLES.....</b>	<b>20</b>
3.2.1 STUDY OF THE ELASTIC MODULUS.....	20
3.2.2 THREE-POINT BENDING TESTS.....	21
3.2.3 HARDNESS TESTING.....	22
<b>3.3. CORROSION ENVIRONMENT: ARTIFICIAL SALIVA - RINGER-HARTMANN SOLUTION.....</b>	<b>22</b>
3.3.1 COMPOSITION OF THE SOLUTION.....	22
3.3.2 REALIZATION OF THE SOLUTION.....	23
<b>3.4 THREE ELECTRODE DEVICE.....</b>	<b>24</b>
3.4.2 FREE POTENTIAL MEASUREMENT: OCP.....	26
3.4.3 OBTENTION OF ELECTROCHEMICAL IMPEDANCE SPECTROSCOPY (EIS).....	27
3.4.4 STUDY OF POLARIZATION CURVES.....	28
<b>3.5 SAMPLE PREPARATION AND ANALYSIS.....</b>	<b>29</b>
3.5.1 CONDUCT OF THE EXPERIMENTS AND DESCRIPTION OF THE ROUTINE.....	30



**CHAPTER 4. RESULTS.....33**

**4.1 STUDY OF CORROSION RESISTANCE.....33**

4.1.1 OCP VALUES OBTAINED.....33

4.1.1.1 OCP VALUES FOR TI35NB.....33

4.1.1.2 OCP VALUES FOR TI35NBXAG.....34

4.1.1.3 OCP VALUES FOR TI35NBXCU.....37

4.1.2 EIS VALUES OBTAINED.....40

4.1.2.1 EIS VALUES OBTAINED FOR TI35NBXCU.....40

4.1.2.2 EIS VALUES OBTAINED FOR TI35NBXAG.....41

4.1.2.3 EIS VALUES OBTAINED FOR TI35NB.....42

4.1.3 POTENTIODYNAMIC CURVE OBTAINED.....43

**CHAPTER 5. DISCUSSION AND ANALYSIS OF RESULTS.....46**

**CHAPTER 6. CONCLUSIONS.....50**

**CHAPTER 7. BIBLIOGRAPHY.....51**

# **DOCUMENT 1**

## **MEMORY**

## INDEX OF FIGURES

<b>Figure 1</b> : Compact hexagonal network form $\alpha$ and centered cubic network $\beta$ .....	15
<b>Figure 2</b> : Diagram of the principle of the three-point bending test (Campus Odontologie, CERIMES, Dr. B. JACQUOT).....	22
<b>Figure 3</b> : Measurement of the PH of the solution with a PH-meter.....	25
<b>Figure 4</b> : Container containing the finish solution.....	25
<b>Figure 5</b> : Potentiostat of work.....	26
<b>Figure 6</b> : Three-electrode assembly used.....	27
<b>Figure 7</b> : Example of obtaining the OCP for the Ti35Nb4Ag alloy.....	28
<b>Figure 8</b> : Example of a polarization curve for Ti35Nb4Ag alloy.....	29
<b>Figure 9</b> : Case containing the samples studied.....	30
<b>Figure 10</b> : Polishing machine used.....	31
<b>Figure 11</b> : Equivalent circuit describing the behavior of the electrode-electrolyte interface...32	
<b>Figure 12</b> : Tafel Slope Method.....	32
<b>Figure 13</b> : OCP values for Ti35Nb alloy.....	34
<b>Figure 14</b> : OCP values for Ti35Nb2Ag.....	35
<b>Figure 15</b> : OCP Values for Ti35Nb4Ag.....	36
<b>Figure 16</b> : OCP Values for Ti35Nb6Ag.....	37
<b>Figure 17</b> : OCP Values for Ti35Nb2Cu.....	38
<b>Figure 18</b> : OCP Values for Ti35Nb4Cu.....	39
<b>Figure 19</b> : OCP Values for Ti35Nb6Cu.....	40
<b>Figure 20</b> : Nyquist diagrams for Ti35NbXCu alloys, representing complex impedance vs. real impedance. ....	41
<b>Figure 21</b> : Bode diagrams for Ti35NbXCu alloys, representing modulus as a function of frequency.....	41
<b>Figure 22</b> : Nyquist diagrams for Ti35NbXAg alloys, representing complex impedance vs. real impedance.....	42
<b>Figure 23</b> : Bode diagrams for Ti35NbXAg alloys, representing modulus as a function of frequency.....	42

<b>Figure 24</b> : Nyquist diagrams for Ti35Nb alloy, representing complex impedance vs. real impedance.....	<b>43</b>
<b>Figure 25</b> : Bode diagrams for Ti35Nb alloy, representing modulus as a function of frequency.....	<b>43</b>
<b>Figure 26</b> : Potentiodynamic curve for copper-containing alloys and alloy reference Ti35Nb.....	<b>45</b>
<b>Figure 27</b> : Potentiodynamic curve for copper-containing alloys and alloy reference Ti35Nb.....	<b>45</b>
<b>Figure 28</b> : Nyquist diagram comparing the studied alloys containing 2% copper or silver.....	<b>47</b>
<b>Figure 29</b> : Nyquist diagram comparing the studied alloys containing 4% copper or silver.....	<b>48</b>
<b>Figure 30</b> : Nyquist diagram comparing the studied alloys containing 6% copper or silver.....	<b>49</b>
<b>Figure 31</b> : Ecorr values as a function of the percentage of Cu or Ag in the alloy.....	<b>50</b>
<b>Figure 32</b> : Icorr values as a function of the percentage of Cu or Ag in the alloy.....	<b>50</b>

## TABLE INDEX

<b>Table 1</b> : Values of the elastic modulus of the working samples.....	<b>21</b>
<b>Table 2</b> : Values of tension of the working samples.....	<b>22</b>
<b>Table 3</b> : Hardness values of working samples.....	<b>23</b>
<b>Table 4</b> : Average OCP value for Ti35Nb.....	<b>34</b>
<b>Table 5</b> : Average OCP value for Ti35Nb2Ag.....	<b>35</b>
<b>Table 6</b> : Average OCP value for Ti35Nb4Ag.....	<b>36</b>
<b>Table 7</b> : Average OCP value for Ti35Nb6Ag.....	<b>37</b>
<b>Table 8</b> : Average OCP value for Ti35Nb2Cu.....	<b>38</b>
<b>Table 9</b> : Average OCP value for Ti35Nb4Cu.....	<b>39</b>
<b>Table 10</b> : Average OCP value for Ti35Nb4Cu.....	<b>40</b>
<b>Table 11</b> : Parameters obtained from the modeling of the electrochemical assembly using a simple circuit represented in Figure 11.....	<b>44</b>
<b>Table 12</b> : Average value of corrosion potential, corrosion current density and polarization resistance for each alloy.....	<b>46</b>

## ABBREVIATIONS

$\alpha$  : Alpha phase

$\beta$  : Beta phase

Ag : Silver

Cu : Copper

CP : Commercially pure

E<sub>corr</sub> : Corrosion potential

I<sub>corr</sub> : Corrosion current density

OCP : Open-Circuit Potential

EIS : Electrochemical Impedance Spectroscopy

R<sub>p</sub> : Polarization resistance

Nb : Niobium

Ti : Titanium

Pt : Platinum

$\chi^2$  Chi-square

# **CHAPTER 1. MOTIVATION AND OBJECTIVES**

## **1.1. MOTIVATION**

With the development of economy and technology, the number of aged people demanding failed tissue replacement is rapidly increasing. Elderly people have a higher risk of hard tissue failure. It is estimated that 70%–80% of biomedical implants are made of metallic materials. Metals and their alloys are widely used as biomedical materials. On one hand, metallic biomaterials cannot be replaced by ceramics or polymers at present. Because mechanical strength and toughness are the most important safety requirements for a biomaterial under load-bearing conditions, metallic biomaterials like stainless steels, Co-Cr alloys, commercially pure titanium (CP Ti) and its alloys are extensively employed for their excellent mechanical properties. On the other hand, metallic materials sometimes show toxicity and are fractured because of their corrosion and mechanical damages. Therefore, development of new alloys is continuously trialed. Purposes of the development are as follows: [1]

- To remove toxic elements
- To decrease the elastic modulus to avoid stress shield effect in bone fixation
- To improve tissue and blood compatibility
- To miniaturize medical devices.

Despite constant improvements due to advances in surgical techniques, subsequent inflammations and infections caused during surgery to implant the replacement biomaterial are still all too common. The problem is particularly marked for dental implants, with a rate of infection (periodontitis) close to 40% [2]. The aim of this work is to analyze the corrosion behavior of 3 types of alloys: the first containing titanium and niobium, the second containing in addition to copper as a third element, and finally silver. Each sample is based on Ti-35Nb because niobium is known to be easily compatible from a biomedical point of view [3]. The choice to work on these elements is not insignificant and was chosen because copper, like silver, are known to be good antibacterial metals that also reduce infections related to dental implants [4,5].

## **1.2. OBJECTIVES**

Objetivo general : The aim of this work is to analyze the behavior of Ti-35NbxCu and Ti-35NbxAg alloys (x =0%, 2%, 4% , 6%) into corrosion environment.

Specific objectives: For this purpose, a classical three-electrode set-up, which will be detailed, will allow to measure different quantities such as OCP (Open-Circuit Potential), EIS (Electrochemical Impedance Spectroscopy) but also the resulting anodic and cathodic curves of each experiment.

# CHAPTER 2. INTRODUCTION

## 2.1. HISTORY OF TITANIUM

Discovered for the first time on the Cornish coast by the Reverend William Gregor in 1790 in black sandy soil, this sand was found in large quantities in the parish of Menachan. It contained 45% of a red metallic substance, soluble in sulfuric acid. Gregor gave it the name menachanite. This menachanite had fallen into oblivion until the German chemist Klaporth (1743-1817) removed it. Indeed, in 1799, Klaporth discovered a new oxide in a sample of red tourmaline from Hungary. He then discovered that this oxide was identical to menachanite. He gave the name titanium: from the modern Latin titanium, derived from Titan. This new metal appeared very difficult to isolate from its compounds. The American Hunter obtained the first quantities of almost pure titanium in 1910 by reducing titanium tetrachloride ( $TiCl_4$ ) with sodium. It was not until 1940 that a Luxembourg chemist, Kroll, developed an industrial production process [6].

### 2.1.1 TWO FORMS OF TITANIUM

Titanium comes in two allotropic forms, i.e. it exists in two different crystal structures,  $\alpha$  and  $\beta$ . The allotropic transformation temperature is between  $882^\circ C$  and  $890^\circ C$  depending on the method of obtaining titanium and the presence of addition elements. Below  $882.5^\circ C$ , titanium is present in its stable, compact or pseudo-compact hexagonal structure  $\alpha$  [6]. Above  $882.5^\circ C$ , the  $\beta$  phase has a stable, centered cubic structure. The temperature of the transitions  $\alpha \leftrightarrow \beta$  is called transus  $\beta$  ( $T_\beta$ ) [7].



Figure 1 : Compact hexagonal network form  $\alpha$  and centered cubic network  $\beta$

Titanium alloys can be of three natures: either they consist only of phase  $\alpha$ , or they consist only of phase  $\beta$ , or they can consist of a mixture of both  $\alpha+\beta$ . It is by mixing titanium with



other elements that different crystal structures can be obtained which can be stabilized at room temperature and allow to

manufacture alloys of the 3 types [6,7]:

- The stabilizing elements  $\alpha$  or alphas, which raise the allotropic transformation temperature (transus  $\beta$ ), are aluminum, oxygen, carbon and nitrogen.
- The stabilizing elements  $\beta$  or betagens, decrease  $T_{\beta}$ . Among these are the eutectoid  $\beta$  elements such as manganese, iron, chromium, silicon, nickel and copper, which can form precipitates.
- Finally, some elements are described as neutral, such as zirconium and tin.

Our study is focused on Ti-35Nb type samples which are  $\beta$  elements, and more precisely beta-isomorphic, i.e. they crystallize in the centered cubic structure and have an atomic radius close to titanium  $\beta$ . This kind of alloy type leads to decrease the elastic modulus to avoid stress shield effect in bone fixation.

This study focuses on Ti-35Nb alloys to which different percentages of copper or silver are added. These two metals were not chosen at random, there are specific reasons for using these two materials. Ag and Cu when alloyed with the Ti matrix, exhibit excellent antibacterial and high corrosion resistance properties. Nb element stands for the upper most alloying element with Ti, which promotes a  $\beta$ -phase in the developed alloys. It helps to reduce the elastic modulus of the implant materials [8].

## 2.2. WHAT THE CORROSION IS?

Corrosion is the action of corroding, destroying slowly, progressively, by chemical action. Corrosion, from the Latin *corrodere*, means to gnaw, to attack. Corrosion is a degradation of the material or its properties by chemical reaction with the environment. This definition admits that corrosion is a harmful phenomenon: it destroys the material or reduces its properties, making it unusable for its intended application.

Another phenomenon that degrades the material is mechanical wear or erosion, the progressive loss of material from the surface of a solid, due to friction or impact. A mainly mechanical phenomenon where, however, chemical interactions between the material and the environment sometimes play a role in the process. important role in speeding up or slowing down degradation. The study of corrosion and protection of metals therefore also includes the degradation phenomena due to combined mechanical and chemical stress.

Sometimes corrosion is a welcome, even desired phenomenon. It destroys and eliminates a large number of objects abandoned in nature. Some industrial processes also involve oxidation. For example, the anodization of aluminum is an oxidation of the metal surface to form a decorative oxide film that protects against atmospheric corrosion. The chemical or electrochemical polishing of metals also makes it possible, by dissolution (corrosion) of the metal, to obtain a smooth and shiny surface. We can therefore give a more general definition of corrosion: corrosion is an irreversible interfacial reaction of a material with its environment, which involves a consumption of the material or a dissolution in the material of a component of the material. the environment [10, 12].

With a few exceptions, metal corrosion is due to an irreversible oxidation-reduction reaction between the metal and an oxidizing agent contained in the environment [6].

## **2.3. THE DIFFERENT TYPES OF CORROSION**

### **2.3.1 NON-AQUEOUS (DRY) CORROSION**

Dry corrosion develops at high temperatures, where certain chemical substances, normally harmless, become corrosive. Among the oxidants responsible for dry corrosion are: oxygen gas, sulfur compounds, anhydride, carbon dioxide (CO<sub>2</sub>) or halogens. In this case there is no passage of electric current. This type of corrosion occurs in the absence of an electrolyte, i.e. in the absence of a conductive medium, is so named as opposed to aqueous corrosion [6,10].

Our work will be carried out in an aqueous medium only. This type of corrosion will therefore obviously not be studied [11,12].

### **2.3.2 AQUEOUS CORROSION**

#### **2.3.2.1 UNIFORM CORROSION**

This is the most common form of corrosion. It corresponds to a relatively regular degradation of the metal over its entire surface [11,12].

#### **2.3.2.2 GALVANIC CORROSION**

This phenomenon occurs when two different metals are in contact within the same electrolyte. The difference in potentials between the two metals is the cause of galvanic corrosion. As two metals do not resist the environment in the same way. When they are put in contact, it is the less noble metal in contact with the electrolyte that will be degraded first [11,12].

#### **2.3.2.3 PITTING CORROSION**

This type of corrosion is localized and mainly affects passivated materials, i.e. protected by a thin oxide layer formed on their surfaces. It is produced by anions, mainly chloride, bromide and iodide ions and an oxidant. The parts concerned by this phenomenon quickly appear perforated with cavities of the order of a few tens of micrometers in diameter, without a large quantity of material necessarily being consumed [11,12].

#### **2.3.2.4 INTERGRANULAR CORROSION**

This form of corrosion is localized at the grain joints [11,12].

#### **2.3.2.5 CORROSION UNDER STRESS OR STRAIN**

Stress corrosion is the association of residual or applied stresses with chemical attack by the environment. This causes small cracks that propagate rapidly and can lead to structural failure [11,12].

#### **2.3.2.6 BACTERIAL CORROSION**

This corrosion occurs due to the presence of bacteria clumping to the surface of the materials. They accumulate acids and dissolved gases, leading to corrosion of the material [11,12].

#### **2.3.2.7 CORROSION BY EROSION AND CAVITATION**

It results from the combined action of an electrochemical reaction and a mechanical removal of material often produced by the rapid movement of a fluid. This can lead to the rupture of passive films and thus cause high corrosion rates on materials normally protected from the environment under static conditions [11,12].

#### **2.3.2.8 STRAY CURRENT CORROSION**

This corrosion phenomenon is caused by poorly insulated electrical installations leading to current leaks in the ground and by the corrosion of parts located within the radius of activity of these stray currents [11,12].

#### **2.3.2.9 SELECTIVE CORROSION (DEALLOYING)**

It results from the preferential dissolution of an alloying element. The material then becomes porous [11,12].

#### **2.3.2.10 CAVERNOUS CORROSION**

Cavernous corrosion results from the formation of an electrochemical cell due to different concentrations of ions or dissolved gases in the electrolyte. These ions and dissolved gases do not access the material in the same way. Crevice corrosion occurs where the concentration of ions and dissolved gases is lowest [11,12].

## **CHAPTER 3. MATERIALS AND METHODS**

### **3.1 MANUFACTURE OF SAMPLES FROM POWDERS**

#### **3.1.1 POWDERS**

The first step in the manufacture of the alloys was to choose the raw material to be used. The powders come from Atlantic Equipment Engineers for Ti and Nb, and from Alfa Aesar for Ag and Cu. The particle size of the powders is an important parameter promoting diffusion during alloy formation. Ti-325 mesh (44  $\mu\text{m}$ ) powders were chosen for titanium. For niobium Nb, smaller particles, between 1 and 5  $\mu\text{m}$ . The particle size chosen for Cu is 0.5 to 1.5  $\mu\text{m}$ , and for Ag is between 0.6 and 2  $\mu\text{m}$ .

Verification of the particle size indicated by the manufacturer was performed using Malvern Instruments' Mastersizer 2000 laser diffraction equipment.

In order to visualize the morphology of the powders with which the work will be carried out, secondary electron images were obtained with the ZEISS AURIGA Compact scanning electron microscope. This results in the observation of a great heterogeneity in the particle morphology for Ti and Nb powders. Cu and Ag powders are more homogeneous [9].

#### **3.1.2 MIXING AND HOMOGENIZATION**

The powders were then mixed in a glove chamber in an argon atmosphere, model GP Campus of the Jacomex company. The powders were then mixed in a glove chamber in an argon atmosphere, model GP Campus of the Jacomex company. Inside the chamber, the different masses needed for each element to form each of the alloys were weighed. The powder mixtures were introduced into plastic containers with three metal balls of 10 mm diameter and sealed with Parafilm. For homogenization and in order to avoid agglomeration of the powders, the mixtures were stirred for 45 minutes at 45 rpm in a 2L inverted tubule, BioEngineering Brand [9].

#### **3.1.3 FORMING OF POWDERS**

After the homogenization process comes the powder compaction. An Instron Model 1343 Universal Hydraulic Press was used for this purpose. To obtain the final shapes, a 30x12x5 mm mold was used. Inside, the quantity of powder was introduced in order to obtain a specimen for each compacting cycle. Zinc stearate was added as a lubricant. The compaction pressure was 700 MPa for all alloy specimens.

After compaction, the resulting samples were characterized and their dimensions measured using a component gauge, which has a sensitivity of 0.01 mm. The masses were measured using a PFB 300 Kern balance with a sensitivity of 0.001 g [9].

#### **3.1.4 SINTERING**

Once the characterization of the specimens was completed, sintering of the compacts was performed to complete the conformation of the samples.

The sintering cycle was followed in a Carbolite vacuum blast furnace, model HVT 15-75-450.

Finally, after obtaining the sintered samples, they were re-characterized in order to calculate the shrinkage undergone by each alloy. Archimedes' principle was used to obtain the porosity of the alloys. To obtain these mass values, a KERN 770 precision balance was used, with a sensitivity of 0.0001 g [9].

### **3.2 SOME PROPERTIES OF WORKING SAMPLES**

For the mechanical characterization of the samples, the following activities or tests are carried out :

- Study of the elastic modulus by means of the pulse excitation technique
- Three-point bending tests
- Hardness testing

#### **3.2.1 STUDY OF THE ELASTIC MODULUS**

The impulse excitation technique is a non-destructive test with which the modulus of elasticity of all samples of each alloy was obtained. The test was performed with Sonelastic® equipment for small samples. An acoustic sensor records the sound signal produced when the specimens are struck with a force controlled by a striker. Five blows, translated into sound signals, in different areas of each specimen were recorded in order to obtain the most accurate average value possible. These signals were processed by the Sonelastic® software in order to obtain the values of the elastic modulus for each repetition [9].

Sample	Elastic Modulus E (Gpa)
Ti35Nb2Cu	81
Ti35Nb4Cu	84
Ti35Nb6Cu	89
Ti35Nb2Ag	71
Ti35Nb4Ag	68
Ti35Nb6Ag	65
Ti35Nb	71

**Table 1** : Values of the elastic modulus of the working samples

There is a significant increase in the modulus of elasticity of the alloys when copper is added to the Ti35Nb base (see table 1). By adding 2% Cu, the average modulus of elasticity increases by 10 GPa. As the percentage of Cu added increases, the modulus of elasticity continues to increase, but less significantly, increasing by 3.5 GPa from 2Cu to 4Cu, and by 5 GPa from 4Cu to 6Cu. It can be seen that the Ti-35Nb-2Ag alloy has an elastic modulus almost identical to that of Ti-35Nb. As the Ag content of the alloys increases, the modulus of elasticity decreases in a non-linear way.

### 3.2.2 THREE-POINT BENDING TESTS

A universal testing machine, Shimadzu's Autograph AG-100 kN Xplus, was used to perform the three-point bending tests. First, the equipment was calibrated, checking references and setting the initial force value to zero. Once the calibration was completed, the applicator applied the force to the sample under study, and an extensometer measured the displacement produced by this force every 0.1 s, recording a pair of force and displacement values at each of these times. These tests were carried out to obtain the parameters necessary for the mechanical characterization of the alloys, such as stress-strain curves and fracture strain. Each specimen broke in two, obtaining two halves with a length between 13 and 15 mm [9].

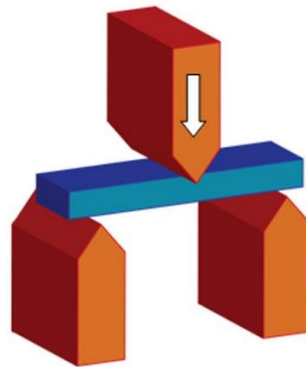


**Figure 2** : Diagram of the principle of the three-point bending test (Campus Odontologie, CERIMES, Dr. B. JACQUOT)

Sample	Tension (Mpa)
Ti35Nb2Cu	385
Ti35Nb4Cu	356
Ti35Nb6Cu	339
Ti35Nb2Ag	403
Ti35Nb4Ag	394
Ti35Nb6Ag	373
Ti35Nb	454

**Table 2 :** Values of tension of the working samples

The results in the table 2, indicate that the alloy with the highest maximum stress value is the control alloy Ti35Nb. It also has the highest strain. It can be seen that the addition of Cu and Ag to the alloy decreases the maximum bending stress, with Cu playing this role more than Ag. The maximum deformation decreases considerably with the addition of Cu to the alloy. However, the addition of Ag causes the strain to decrease much more slightly.

### 3.2.3 HARDNESS TESTING

In order to determine the hardness of each alloy, five indentations were made on each sample with a Rockwell Ball Penetrator 980 N. The load on each indentation was applied for 15 s. The durometer used was that of Centaur, model HD9-45 [9]. The table 3 shows these results.

Sample	Hardness Vickers (HV)
Ti35Nb2Cu	136.1
Ti35Nb4Cu	138.8
Ti35Nb6Cu	140.2
Ti35Nb2Ag	123.1
Ti35Nb4Ag	122.5
Ti35Nb6Ag	121.6
Ti35Nb	126.4

**Table 3 :** Hardness values of working samples



### **3.3. CORROSION ENVIRONMENT: ARTIFICIAL SALIVA - RINGER-HARTMANN SOLUTION**

#### **3.3.1 COMPOSITION OF THE SOLUTION**

The corrosion tests were all carried out in an aqueous medium, in artificial saliva. The aim was to get as close as possible to the real conditions, i.e. the composition of human saliva in order to follow the evolution of the samples and their corrosion resistance in an oral environment.

For this purpose, Ringer-Hartmann artificial saliva was chosen because it is considered to be very representative of real saliva. This solution was each time realized for a volume of 1 liter, here is the detail of its composition :

- Sodium Chloride NaCl : 6g
- Potassium Chloride KCl : 0,3718g
- Calcium Chloride CaCl<sub>2</sub> : 0,2297g
- Lactate : 5,146ml

#### **3.3.2 REALIZATION OF THE SOLUTION**

The realization of the solution was a meticulous work because it was necessary to take care to respect as exactly as possible the quantities of each component in order to have, with each new realization of the solution, an identical composition of the saliva during the experiments.

In a large beaker previously filled with distilled water (about 0.75L), the products listed above were introduced one by one. Each product was weighed on a precision scale in order to respect the predefined quantities as precisely as possible. Then to these products put, then mixed in the large beaker was added 5.146ml of Lactate.

This solution was then transferred to a 1L flask which was topped up with distilled water to reach the exact volume.

Finally, once the solution is well diluted after mixing, it is poured into a container. A small quantity of the solution is taken in order to measure its PH. This measurement is taken daily to ensure that the PH remains approximately constant within a range of 6 to 7.2. Figure 3 and 4 show how the PH has been measured, and where the solution has been contained.

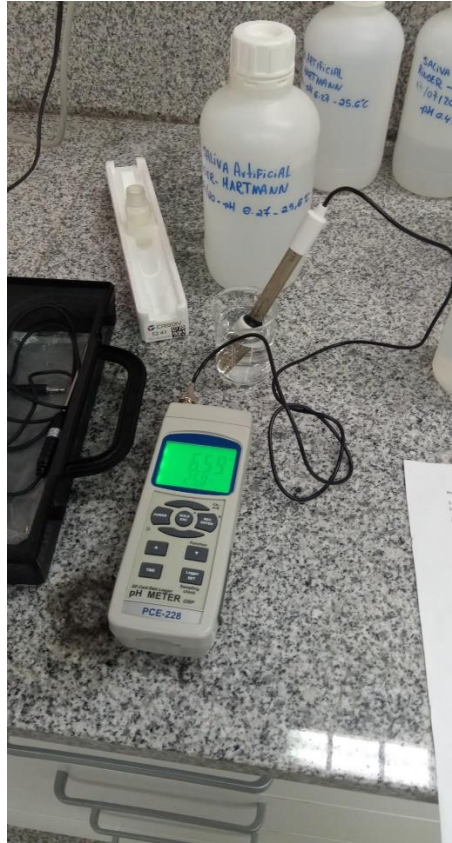


**Figure 3 :** Measurement of the PH of the solution with a PH-meter

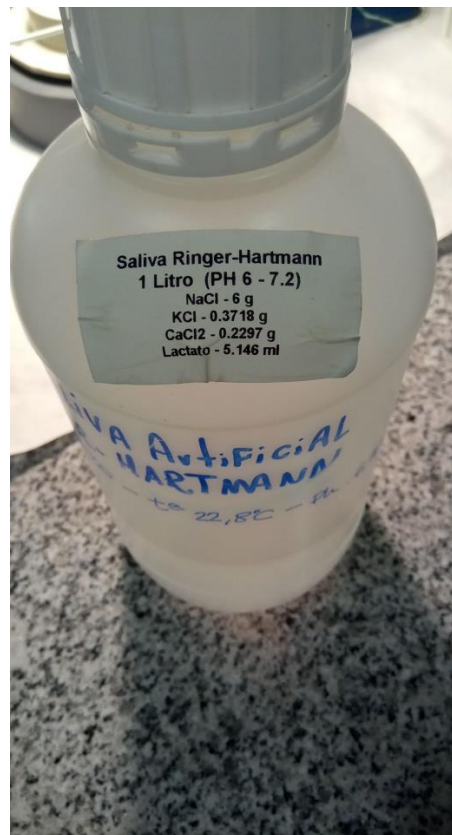


**Figure 4 :** Container containing the finish solution

Generally, at 25 degrees, the measured PH was between 6.6 and 6.72 for all experiments.

### 3.4 THREE ELECTRODE DEVICE

Corrosion tests were carried out by means of electrochemical measurements. The apparatus used is a potentiostat type AUT51095 AUTOLAB, connected to a computer containing the Nova 2.1.4 software, allowing the obtaining and analysis of the results.



**Figure 5 :** Potentiostat of work

The potentiostat is connected to an electrochemical cell consisting of three electrodes: the working electrode, the reference electrode and the auxiliary electrode.

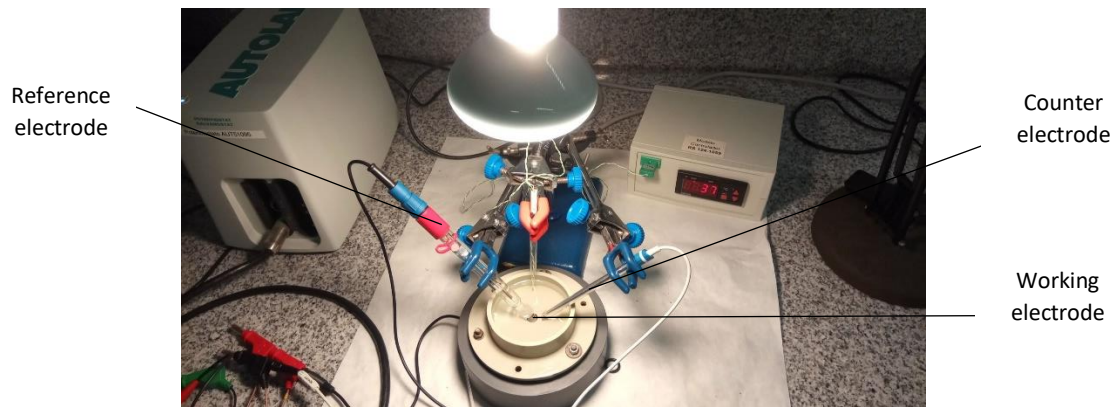


**Figure 6:** Three-electrode assembly used

The potentiostat imposes a potential difference between the working electrode and the reference electrode and measures the current between the auxiliary electrode and the working electrode.

- The working electrode corresponds to the material to be electrochemically characterized, more precisely, it is an electrochemical interface. This material is a sample that has been previously polished and cleaned (preparation process explained below).
- The reference electrode used was the Ag/AgCl electrode from Metrohm AUTOLAB
- The auxiliary electrode, also called the counter electrode, is a platinum electrode. It ensures the passage of current through the cell and thus makes it possible to modulate the flow of electrons and thus the intensity of the electrochemical reactions that occur on the surface of the working electrode.

All the experiments were carried out using this set-up, the electrolyte used being of course Ringer-Hartmann artificial saliva, the composition of which was developed in the previous chapter. Corrosion tests were conducted at room temperature (25°C) under static conditions, i.e. with fixed electrodes on a support and without mixing the solution. The solution is systematically changed before starting a new test in order to avoid the possible presence of residual ionic particles from the previous measurement.

### **3.4.2 FREE POTENTIAL MEASUREMENT: OCP**

The resistance of titanium and its alloys to corrosion in a medium is related to the quality of the layer of oxide film formed when they are placed in that medium. This layer must be both uniform and stable. The OCP (Open Circuit Potential) is the equilibrium potential of the material in the absence of electrical connections on the material. It is also called free potential.

The aim is to evaluate the physico-chemical properties of the titanium alloy in the Ringer-Hartmann solution prepared beforehand for a given period of time. The idea being to evaluate the electrochemical corrosion behavior of the oxide film, it is necessary to allow sufficient time for the OCP to stabilize before starting an electrochemical measurement. An increase in potential at the beginning of the measurement represents the formation of the passivation layer

consisting of titanium oxides. Then a slower increase in potential shows the growth of the oxide film on the surface of the titanium alloy [11].

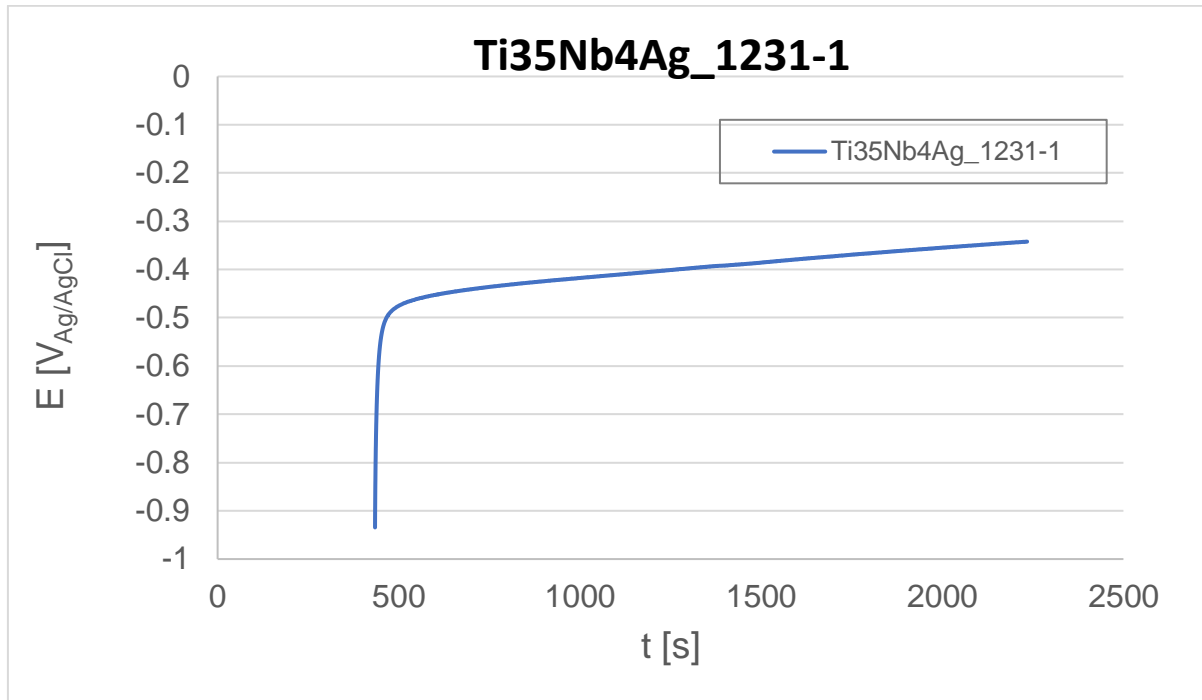


**Figure 7** : Example of obtaining the OCP for the Ti35Nb4Ag alloy

During an OCP measurement, we obtain a graph representing the potential as a function of the measurement time. In the example in Figure 7, the OCP measurement starts at 475 seconds. Before that, a step called Cathodic Cleaning takes place ( it consists in applying a potential of -1V during this time before the start of the measurement). It can be seen that after a certain time the potential reaches equilibrium and the OCP value for the alloy under investigation can be obtained. Here, the OCP value for the alloy, whose specimen number is 1231, is -0.34 V.

### 3.4.3 OBTENTION OF ELECTROCHEMICAL IMPEDANCE SPECTROSCOPY (EIS)

Electrochemical impedance spectroscopy consists in measuring the response of an electrode to a low amplitude sinusoidal potential modulation at different frequencies. The response obtained consists of an impedance value, with a real part and a complex part, for each of the frequency values studied. With these parameters, Nyquist and Bode diagrams will be obtained for each alloy. Finally, the EIS experimental data will be modeled using an equivalent electrical circuit composed of passive elements. The diagrams and parameters obtained from the model will help us to interpret the electrochemical behavior of our alloys.

### 3.4.4 STUDY OF POLARIZATION CURVES

Potentiodynamic polarization curves are graphs that relate the potential ( $E$ , in V), to the current density ( $i$ , in  $A/cm^2$ ) on the working electrode.

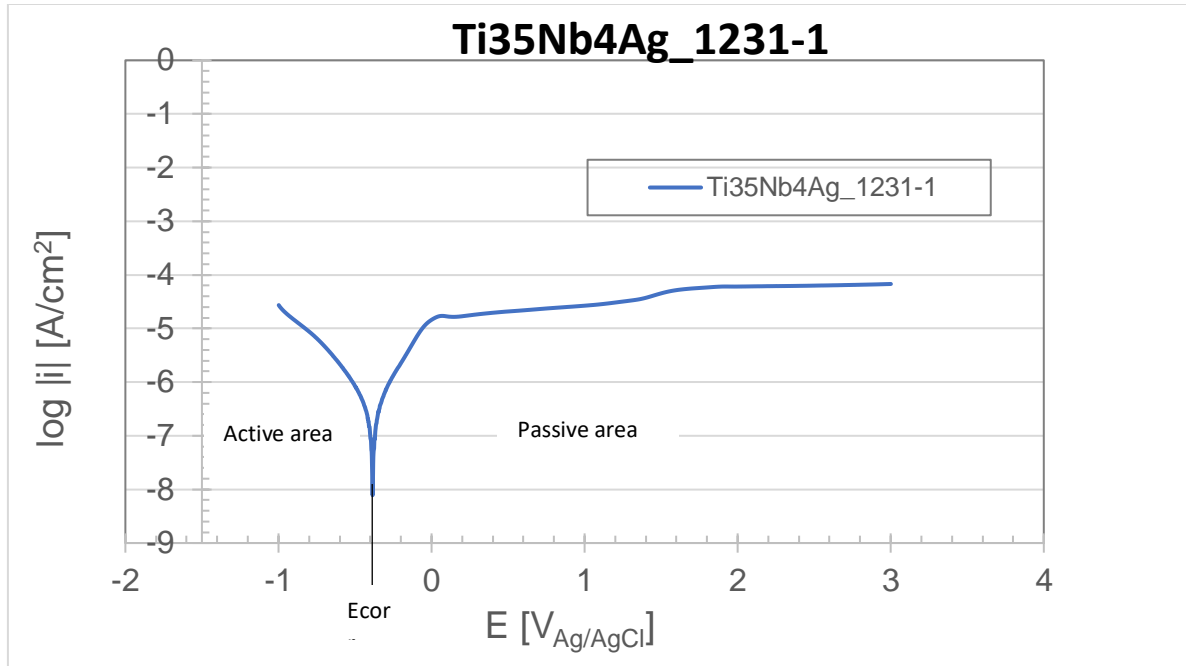


**Figure 8 :** Example of a polarization curve for Ti35Nb4Ag alloy

To obtain these curves, a potential scan from the OCP value to -1V (cathode zone) and then from -1V to 2V (anode zone) will be performed at a scan rate of 0.002 V/s. It is essential that this sweep rate be as slow as necessary to take into account the conditions of the ground transport state on the electrode Surface [12].

The parameters that we will obtain from these curves to characterize the corrosion resistance of alloys are :

- Corrosion potential ( $E_{corr}$ ): equilibrium potential between the working and reference electrodes.
- Corrosion current density ( $I_{corr}$ ): value of the current density for the value of the potential equal to  $E_{corr}$ .
- Polarization resistance ( $R_p$ ): Slope of the potentiodynamic curve at potentials close to equilibrium.

### 3.5 SAMPLE PREPARATION AND ANALYSIS

The samples were obtained by the process explained in part 2.3. There are therefore seven samples of different nature (Ti35NbXCu, Ti35NbYAg and Ti35Nb, where X and Y are 2, 4 or 6).



**Figure 9 :** Case containing the samples studied

Before the start of each experiment, the sample must be prepared in the same way each time so that the preparation does not influence the results in any way.

Therefore, first of all, it is necessary to polish the sample.

On a GP-1B Grinder Polisher polishing machine of the brand Polirresin, the specimen is polished using a Struers brand glass sheet type FEPA P #500 with a grain size of 30  $\mu\text{m}$ . Next, a FEPA P #1000 type sheet is used where the grain size is 18  $\mu\text{m}$ . Finally, to complete the polishing process, a FEPA P #3000 sheet is used, containing 6 $\mu\text{m}$  grains.

After polishing, the sample is immersed in a beaker containing a mixture of ethanol and acetone, itself immersed in a water bath at 35°C for 10 minutes.



**Figure 10** : Polishing machine used

Following this preparation, the sample can finally be analyzed in the 3-electrode device detailed in the previous section 4.1. These analyses give OCP and EIS measurements as well as information on polarization curves, the subject of the next part.

### **3.5.1 CONDUCT OF THE EXPERIMENTS AND DESCRIPTION OF THE ROUTINE**

The potentiostat used in these tests was AUTOLAB's model AUT51095, its function is to maintain a constant potential between the working electrode and the reference electrode. The working electrode, as already mentioned in the survey planning, is the sample. The reference electrode used was the Ag/AgCl electrode from Metrohm AUTOLAB and the counter electrode used was a Pt electrode from Radiometer Analytical. The working area, or exposed surface of the sample, was a circle with a radius of 0.5 cm, with a total surface area of 0.785 cm<sup>2</sup>. The electrolyte on which the tests were performed was artificial saliva of the Ringer-Hartmann type. The artificial saliva was kept at 37°C for the duration of the test by a halogen lamp, in order to simulate the conditions of the human body. A thermocouple will be used to control the temperature.

The routine to be performed takes a total time of about two hours. During this time, the NOVA software obtains the open circuit potential (OCP), the electrochemical impedance spectroscopy (EIS) and the potentiodynamic, cathodic and anodic curves.

First of all, the OCP value is obtained thirty minutes after the experiment is started.



With a potential value equal to the OCP, electrochemical impedance spectroscopy (EIS) was obtained. A sine wave with an amplitude of 0.01 V was used to determine the impedance value for frequency values between 0.005 and 100,000 Hz. From these impedance values at different frequencies, Nyquist (impedance versus less complex impedance) and Bode (impedance modulus versus frequency, and impedance phase versus frequency) diagrams are obtained.

To finally understand the variation of impedance with frequency, our electrochemical assembly will be modeled using an equivalent circuit. This is a circuit composed of a capacitor and a resistor connected in parallel, which describes the electrical behavior of the electrode-electrolyte interface, adding in front of them a resistor representing the ohmic drop of the electrolyte between the reference and working electrodes.

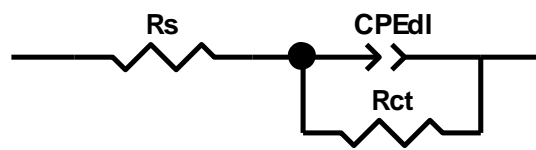


**Figure 11 :** Equivalent circuit describing the behavior of the electrode-electrolyte interface

For the potentiodynamic cathodic curve, current density values are obtained for potential values from OCP to -1V, with a step of 0.002 V/s. The anodic potentiodynamic curve was obtained by recording current density values from -1V to 2V, also with a step of 0.002 V/s. From these curves, we will obtain two fundamental parameters for the characterization of the corrosion resistance of alloys, the corrosion potential ( $E_{corr}$ ) and the corrosion current density ( $i_{corr}$ ). These parameters have been calculated using the Tafel slope method.

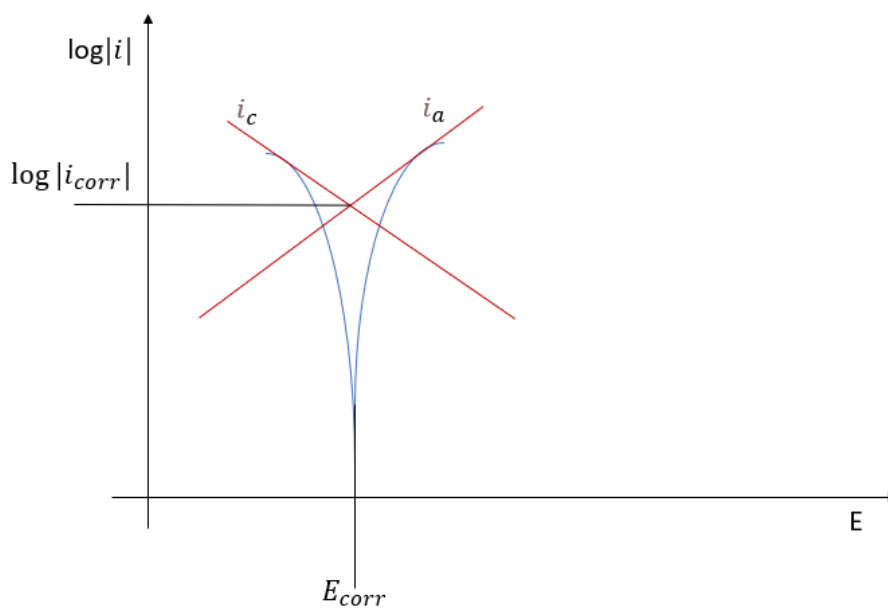


**Figure 12 :** Tafel Slope Method

This method was performed by the Mathematica software which gave the values of  $E_{corr}$ ,  $i_{corr}$  and  $R_p$ .

# CHAPTER 4. RESULTS

## 4.1 STUDY OF CORROSION RESISTANCE

### 4.1.1 OCP VALUES OBTAINED

#### 4.1.1.1 OCP VALUES FOR TI35NB

The following diagrams and figures represent the values obtained in the experiments. These results were obtained under exactly the same conditions for each of them. However, it should be noted that for the same sample, the values obtained are not exactly the same each time. These discrepancies will be discussed in the next chapter, which will interpret and explain the results.

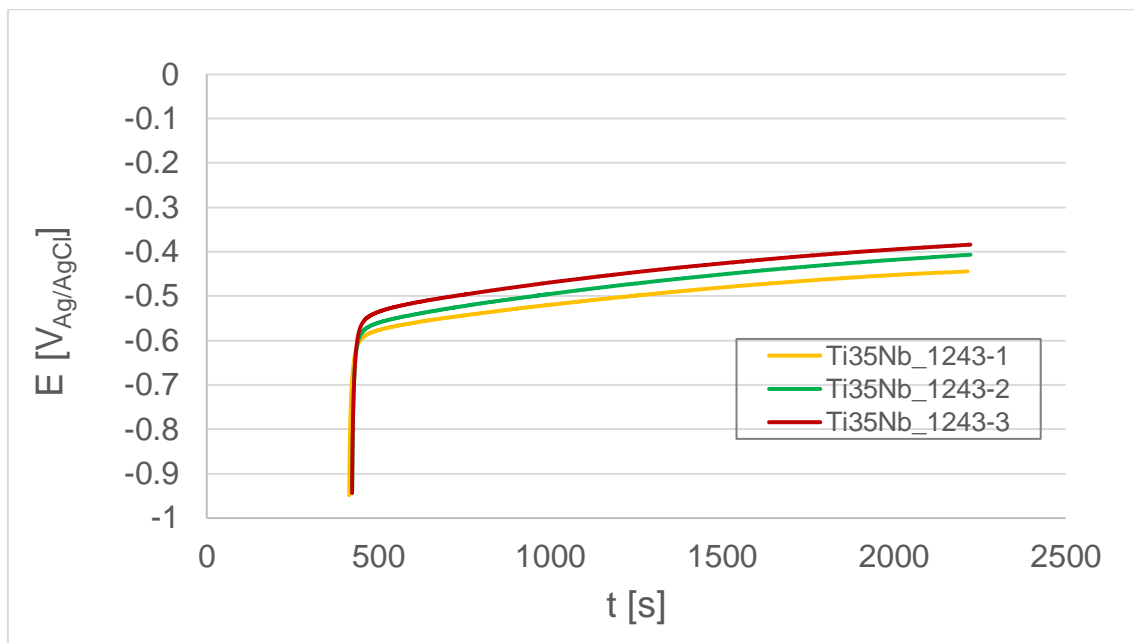


**Figure 13** : OCP values for Ti35Nb alloy

These are the Open-Circuit Potential values for the reference alloy Ti35Nb, i.e. the alloy containing only titanium and niobium. For each measurement, 3 experiments were carried out. The OCP gives us the equilibrium potential of the material in the absence of electrical connections on the material.

This is the sample that shows the most consistent results during the experiments. Here is the table 4 which groups the three values obtained and the calculated average.

OCP - Ti35Nb			
Sample	OCP (V)	av. OCP (V)	±
1243-1	-0,44	<b>-0,41</b>	0,03
1243-2	-0,41		
1243-3	-0,38		

**Table 4 :** Average OCP value for Ti35Nb

The results obtained for the Ti35Nb alloy will serve as a reference and basis for the analysis of the results, as the following results concern samples to which copper or silver is added in different quantities.

#### 4.1.1.2 OCP VALUES FOR TI35NBXAG

The figure 14 shows the OCP values for Ti35Nb2Ag alloy. Contrary to the others, four measurements were made since an error in one of the tests (in the 1222-2, the red one) had occurred.

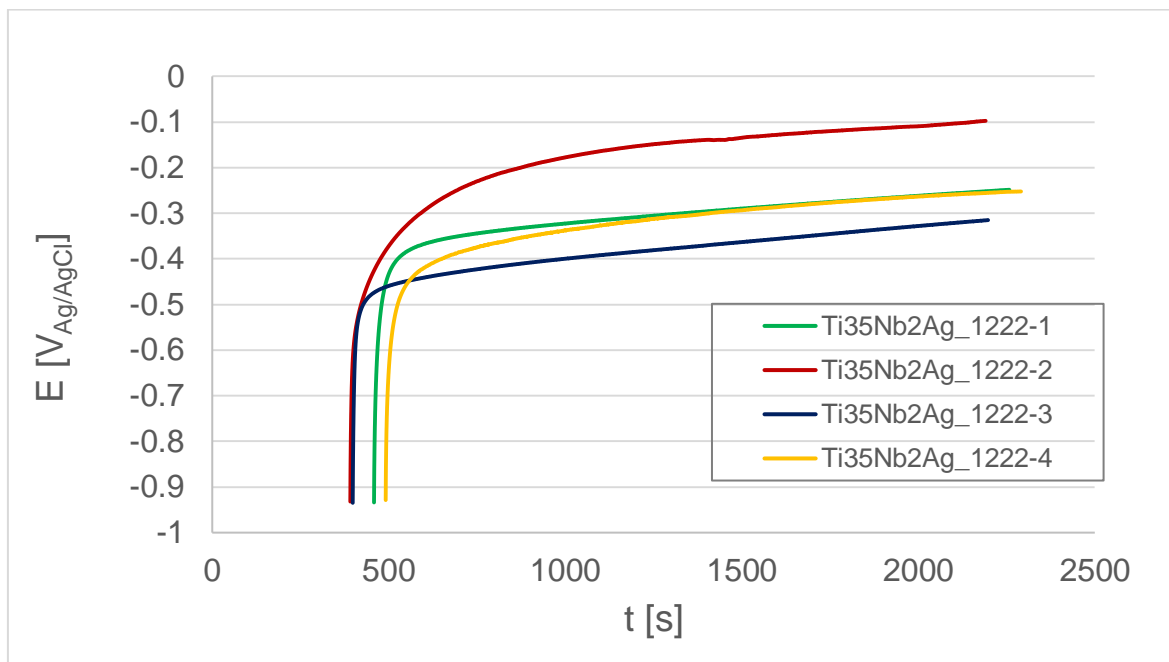


**Figure 14 :** OCP vallues fot Ti35Nb2Ag

OCP – Ti35Nb2Ag			
Sample	OCP (V)	av. OCP (V)	±
1222-1	-0,25	<b>-0,27</b>	0,04
1222-3	-0,32		
1222-4	-0,25		

**Table 5 :** Average OCP value for Ti35Nb2Ag

This figure 15 shows OCP values for a Ti35Nb4Ag alloy.

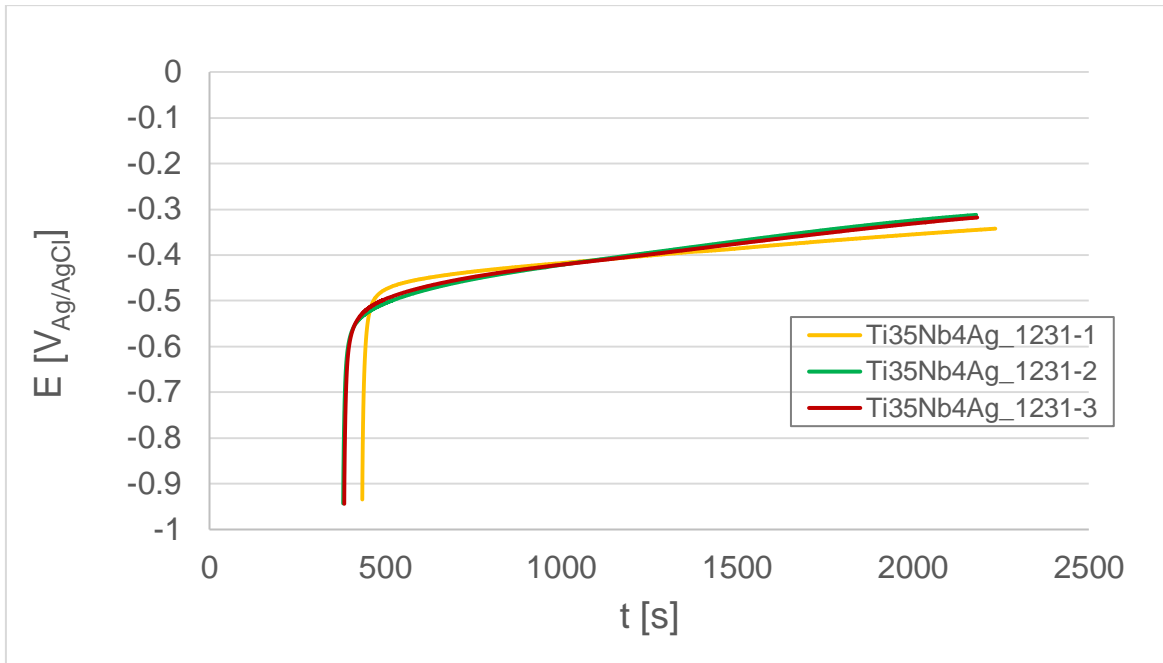


**Figure 15 :** OCP Values for Ti35Nb4Ag

OCP - Ti35Nb4Ag			
Sample	OCP (V)	av. OCP (V)	±
1231-1	-0,34	<b>-0,32</b>	0,02
1231-2	-0,31		
1231-3	-0,32		

**Table 6 :** Average OCP value for Ti35Nb4

Finally, these are the values for Ti35Nb6Ag alloy, in the figure 16.

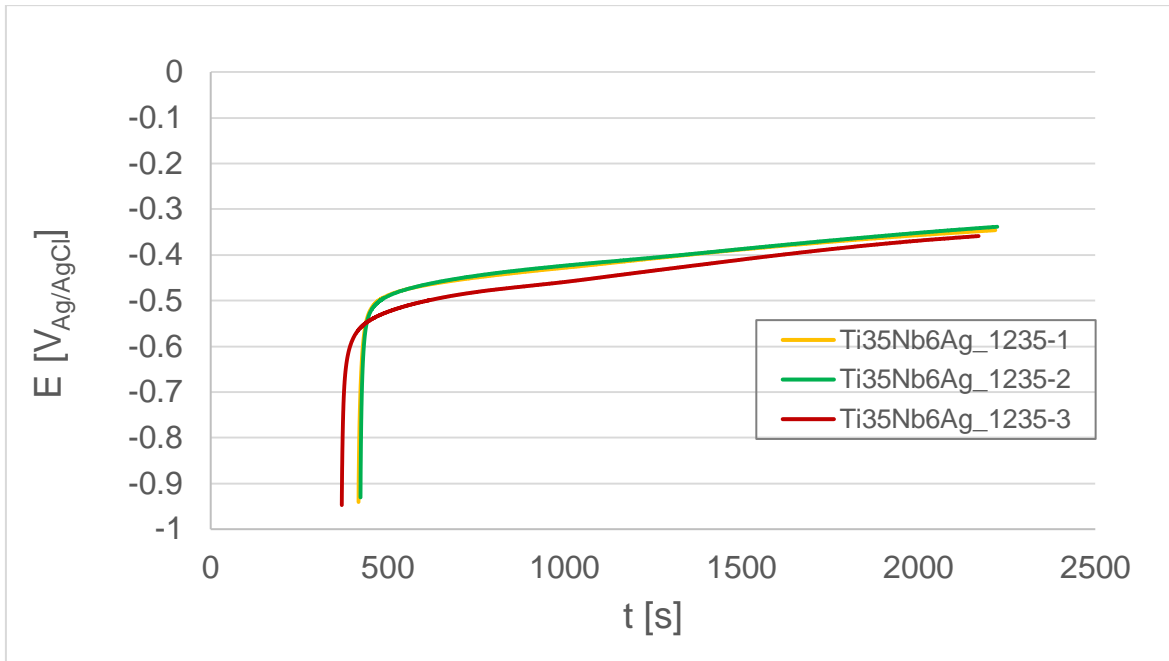


**Figure 16** : OCP Values for Ti35Nb6Ag

OCP - Ti35Nb6Ag			
Sample	OCP (V)	av. OCP (V)	±
1235-1	-0,34	-0,35	0,01
1235-2	-0,34		
1235-3	-0,36		

**Table 7** : Average OCP value for Ti35Nb6

A first observation can already be made. The absolute value of OCP increases the higher the percentage of silver in the alloy. It even tends to approach the average OCP value for the reference alloy which is Ti35Nb. Now, OCP results for copper-containing alloys will be presented.

#### 4.1.1.3 OCP VALUES FOR Ti35NBXCU

The results presented in this section concern copper-containing alloys. It will be interesting to note that the results of the experiments are more disparate than for any other alloy. For example, as shown in Figure 17, the first experiment is totally out of phase with the other two results. It will therefore not be taken into account in the calculation of the average.

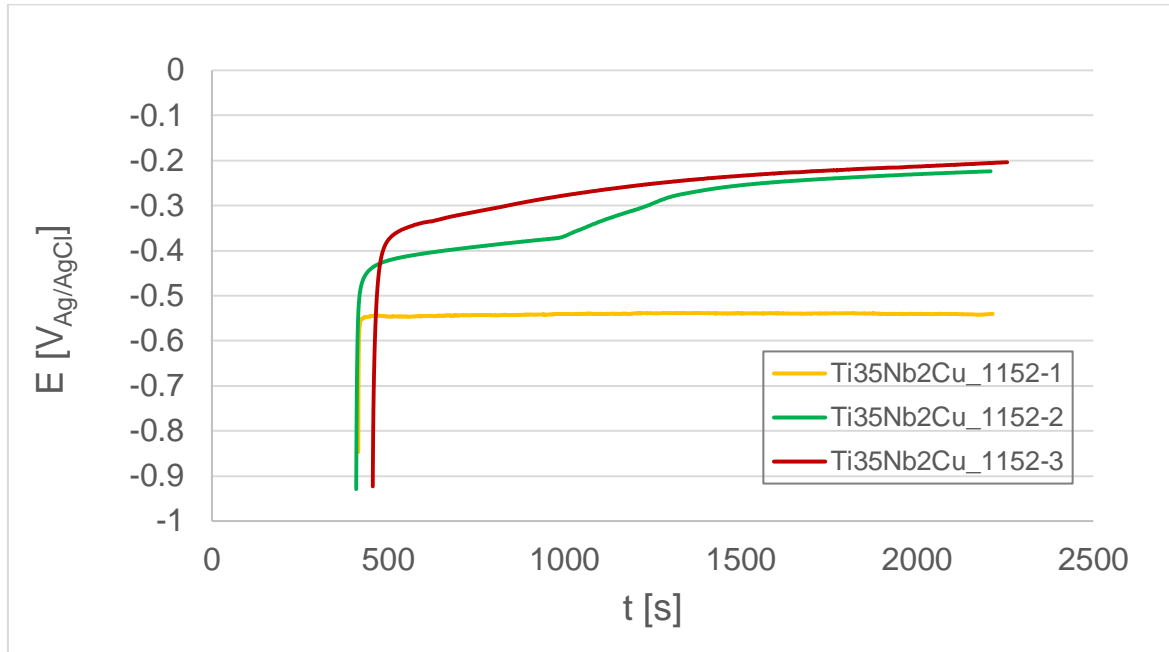


Figure 17 : OCP Values for Ti35Nb2Cu

OCP - Ti35Nb2Cu			
Sample	OCP (V)	av. OCP (V)	±
1152-1	-0,54	-0,21	0,19
1152-2	-0,22		
1152-3	-0,20		

Table 8 : Average OCP value for Ti35Nb2Cu

As shown in the table, the first value obtained is far removed from the other two, which suggests the idea that an event disrupted the course of the experiment.

The results are more homogeneous (see figure 18) for the Ti35Nb4Cu alloy but not as homogeneous as for the previous alloys containing silver.

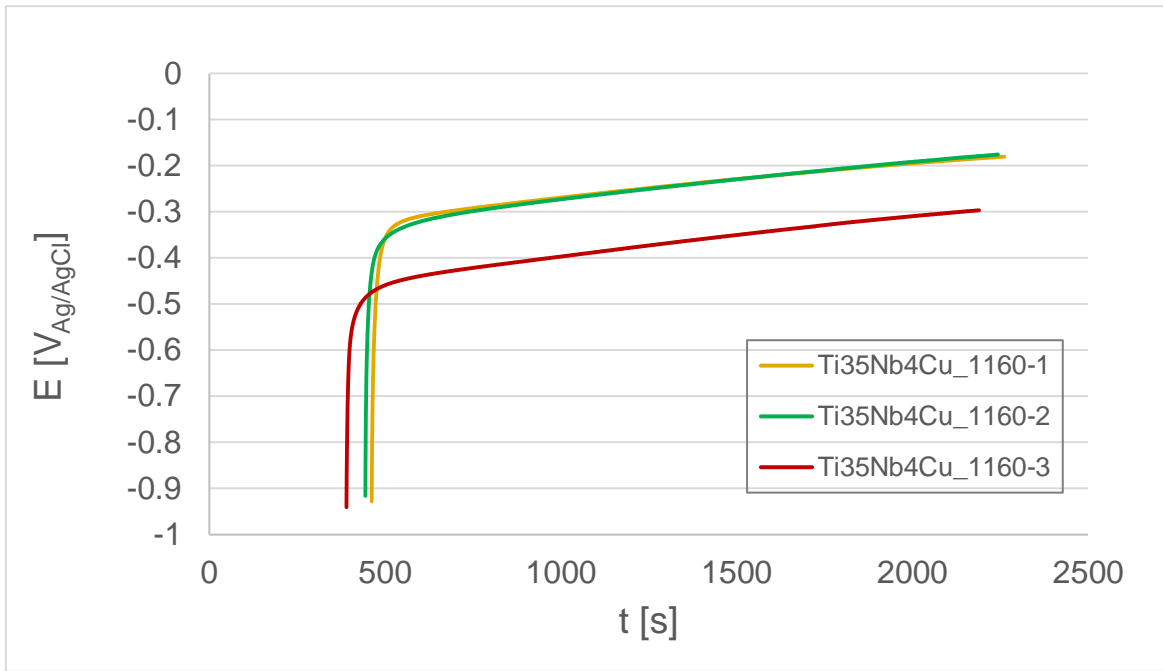


**Figure 18** : OCP Values for Ti35Nb4Cu

OCP - Ti35Nb4Cu			
Sample	OCP (V)	av. OCP (V)	±
1160-1	-0,18	-0,21	0,07
1160-2	-0,17		
1160-3	-0,29		

**Table 9** : Average OCP value for Ti35Nb4Cu



Finally, here are the results obtained for the Ti35Nb6Cu sample.(see figure 19 and table 10)

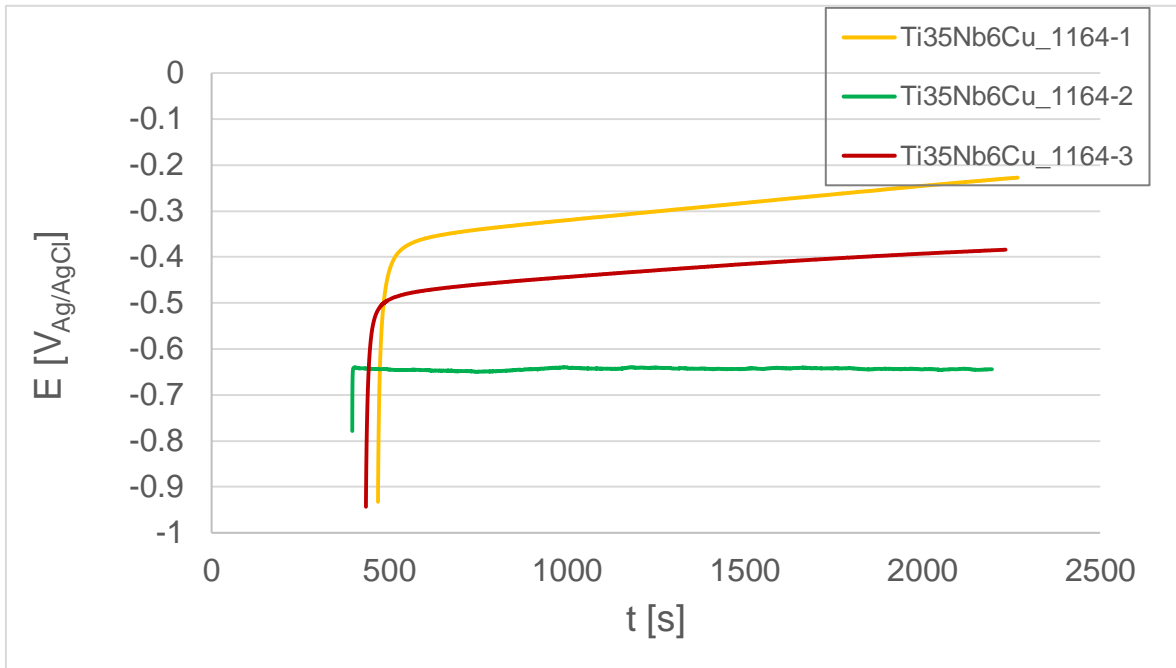


Figure 19 : OCP Values for Ti35Nb6Cu

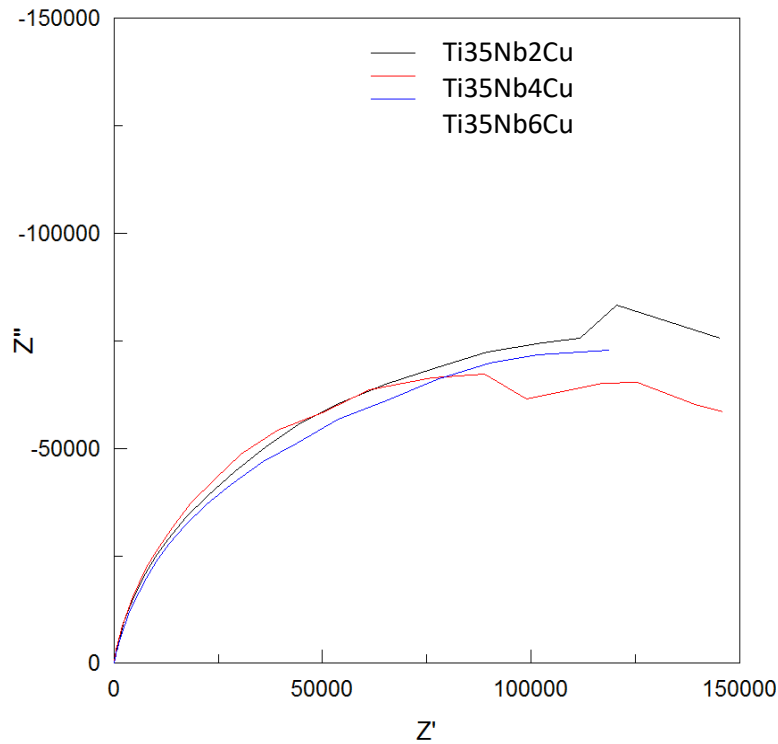
OCP - Ti35Nb6Cu			
Sample	OCP (V)	av. OCP (V)	±
1164-1	-0,23	-0,42	0,21
1164-2	-0,64		
1164-3	-0,38		

Table 10 : Average OCP value for Ti35Nb4Cu

#### 4.1.2 EIS VALUES OBTAINED

From electrochemical impedance spectroscopy (EIS), Nyquist and then Bode diagrams of the studied alloys were obtained using Zview software. EIS measurement is used to measure the transfer resistance of the reaction, the capacity of the interfacial double layer capacitor and the electrolyte resistance.

##### 4.1.2.1 EIS VALUES OBTAINED FOR Ti35NbXCu



**Figure 20** : Nyquist diagrams for Ti35NbXCu alloys, representing complex impedance vs. real impedance.

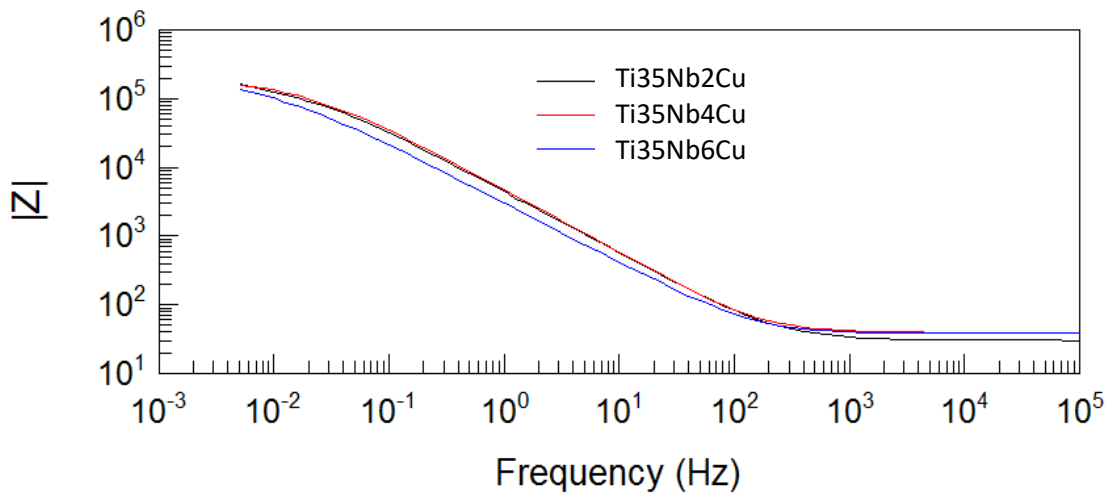


**Figure 21** : Bode diagrams for Ti35NbXCu alloys, representing modulus as a function of frequency.

#### 4.1.2.2 EIS VALUES OBTAINED FOR Ti35NbXAg

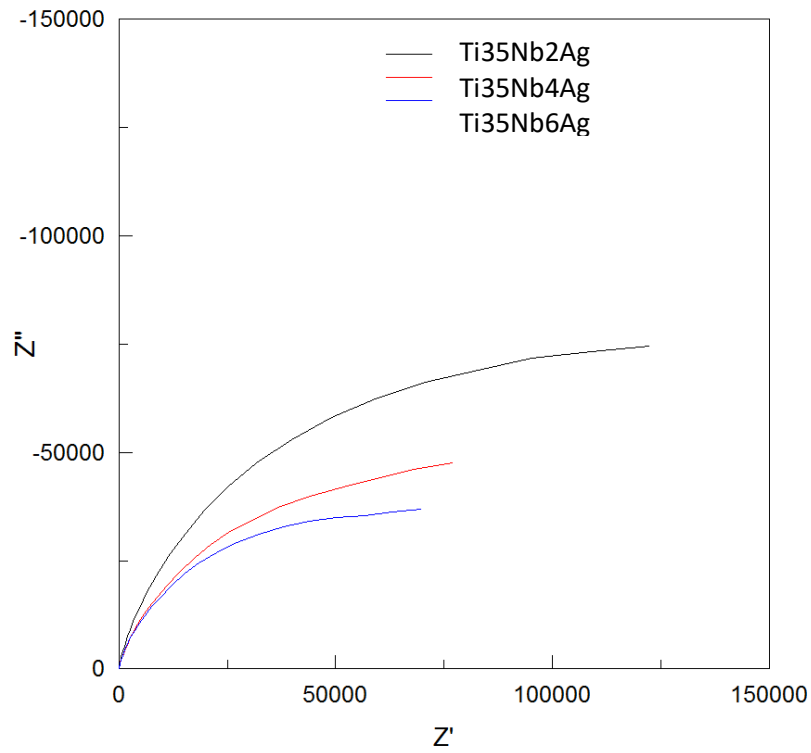


**Figure 22 :** Nyquist diagrams for Ti35NbXAg alloys, representing complex impedance vs. real impedance.

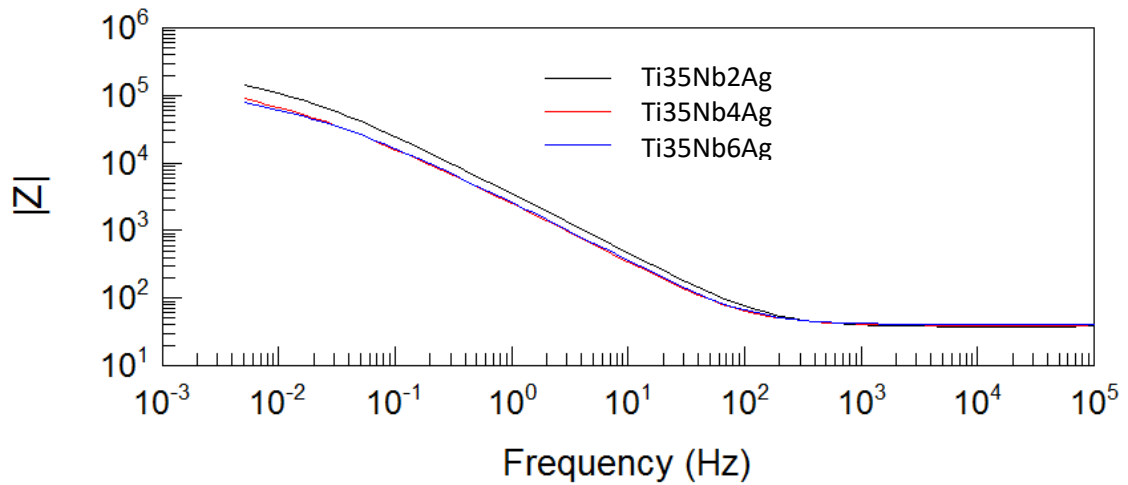


**Figure 23 :** Bode diagrams for Ti35NbXAg alloys, representing modulus as a function of frequency.

#### 4.1.2.3 EIS VALUES OBTAINED FOR TI35NB

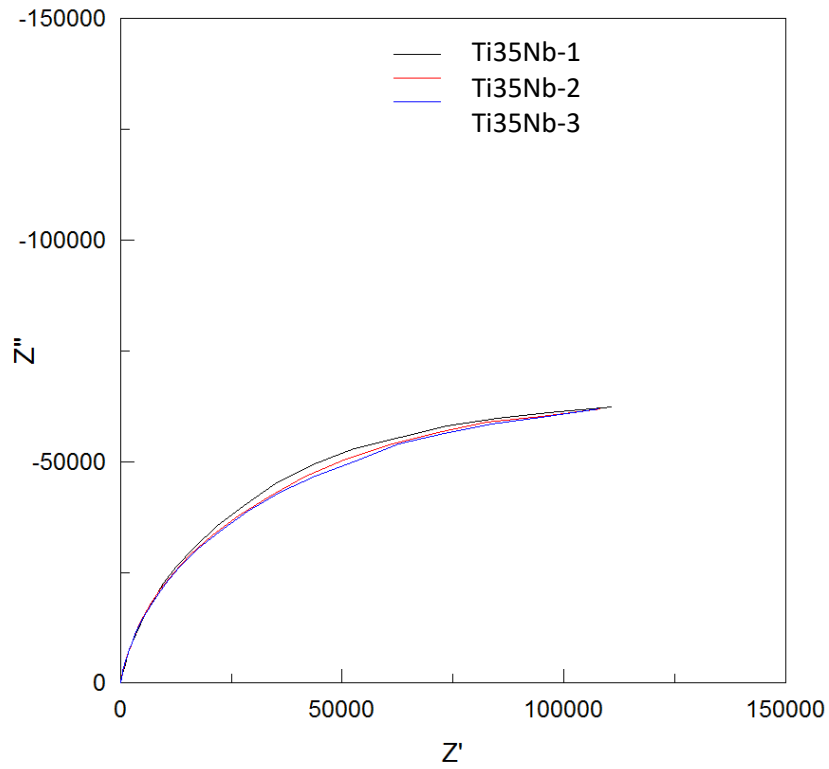


**Figure 24 :** Nyquist diagrams for Ti35Nb alloy, representing complex impedance vs. real impedance.

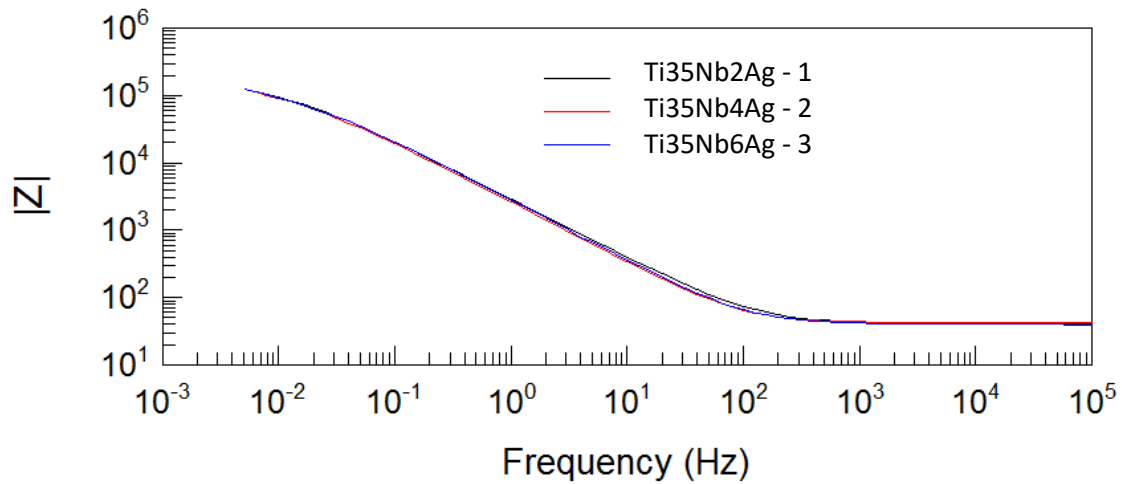


**Figure 25 :** Bode diagrams for Ti35Nb alloy, representing modulus as a function of frequency.

The following table shows the average of some of the values obtained in the EIS tests :

- **Rs** is the resistance - the ohmic drop of the electrolyte between the reference and working electrodes.
- **Rct** is resistance associated with the porous metal layer
- **CPEdl** is the capacitor which, in parallel with the resistor Rct, describes the electrical behavior of the electrode-electrolyte interface.
- $\chi^2$  Chi-square value obtained for model fitting.

	<b>Rs(<math>\Omega \cdot \text{cm}^2</math>)</b>	<b>Rct(<math>\text{k}\Omega \cdot \text{cm}^2</math>)</b>	<b>CPEdl(<math>\mu\text{F}/\text{cm}^2</math>)</b>	<b><math>\chi^2</math></b>
<b>Ti35Nb2Cu</b>	34,9	90,3	51,1	4,5 exp-1
<b>Ti35Nb4Cu</b>	43,1	167,3	42,3	2,5 exp0
<b>Ti35Nb6Cu</b>	36,8	159,5	72,4	0,6 exp0
<b>Ti35Nb2Ag</b>	39,9	158,6	50,0	0,2 exp-1
<b>Ti35Nb4Ag</b>	39,2	93,8	73,2	0,6 exp-2
<b>Ti35Nb6Ag</b>	39,5	92,5	88,5	0,3 exp-2
<b>Ti35Nb</b>	40,9	130,9	73,0	0,4 exp-2

**Table 11** : Parameters obtained from the modeling of the electrochemical assembly using a simple circuit represented in Figure 11.

As can be seen in the table, the electrical model used is much more suitable for silver-containing alloys, or the reference Ti35Nb alloy, than for copper-containing alloys, as indicated by the chi-square values. Indeed, the lower the chi-square values, the better the compatibility between the theoretical model and the practical results.

#### 4.1.3 POTENTIODYNAMIC CURVE OBTAINED

Finally, the potentiodynamic curves are presented. The parameters obtained from them using the Mathematica software provide a lot of information to know the corrosion behaviour of alloys. From these potentiodynamic curves are obtained the corrosion potential ( $E_{\text{corr}}$ ), the corrosion current density ( $i_{\text{corr}}$ ) and the polarization resistance ( $R_p$ ).

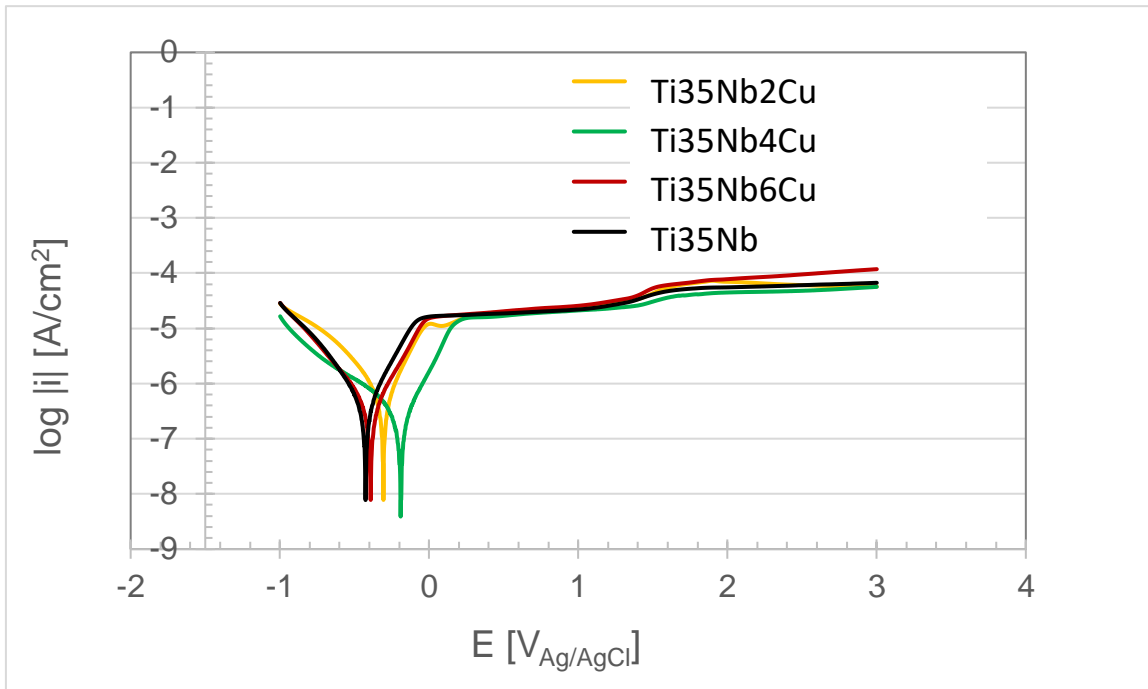


**Figure 26 :** Potentiodynamic curve for copper-containing alloys and alloy reference Ti35Nb

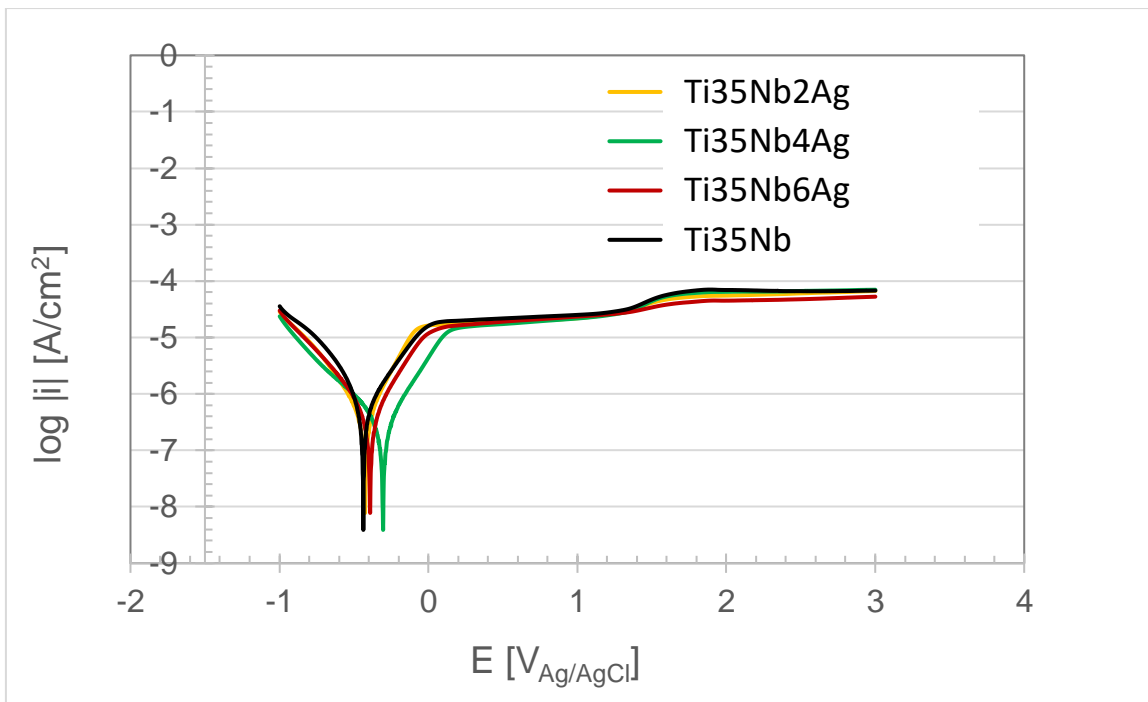


**Figure 27 :** Potentiodynamic curve for copper-containing alloys and alloy reference Ti35Nb

It can be seen from these graphs that the higher the silver percentage, the more the curves tend to move towards the left, towards the control curve of the Ti35Nb alloy. The same phenomenon can be observed with alloys containing copper with the difference that it is the alloy containing 4% copper that is the most to the right. These observations are confirmed by the numerical results obtained, detailed in the following table.

	<b>E<sub>corr</sub> (V)</b>	<b>I<sub>corr</sub> (A /cm<sup>2</sup>)</b>	<b>R<sub>p</sub> (kΩ)</b>
<b>Ti35Nb2Cu</b>	-0,27	1,7.exp-7	176
<b>Ti35Nb4Cu</b>	-0,18	0,9.exp-7	250
<b>Ti35Nb6Cu</b>	-0,32	1,2.exp-7	238
<b>Ti35Nb2Ag</b>	-0,36	0,8.exp-7	239
<b>Ti35Nb4Ag</b>	-0,38	1,5.exp-7	172
<b>Ti35Nb6Ag</b>	-0,42	1,0.exp-7	145
<b>Ti35Nb</b>	-0,43	1,6.exp-7	169

**Table 12 :** Average value of corrosion potential, corrosion current density and polarization resistance for each alloy.

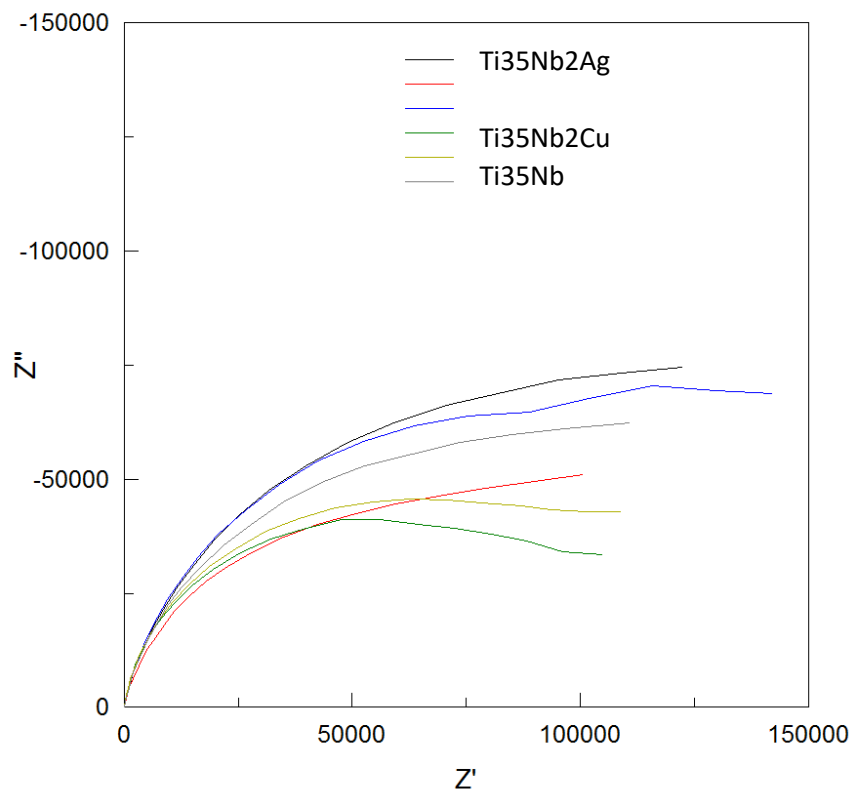
These results are in line with what has been shown in the previous figures. The corrosion potential of silver-containing alloys tends to approach that of Ti35Nb alloy as the silver content increases. The same applies to the corrosion current density.

## CHAPTER 5. DISCUSSION AND ANALYSIS OF RESULTS

Titanium is an element with high corrosion resistance. In addition, several authors have shown that the addition of Niobium to the alloy improves the resistance to electrochemical corrosion, compared to Ti CP or Ti6Al4V alloy [13,14,15]. The various results obtained with the addition of Copper and Silver to this Ti35Nb base will tell us whether or not it is beneficial to add these metals.

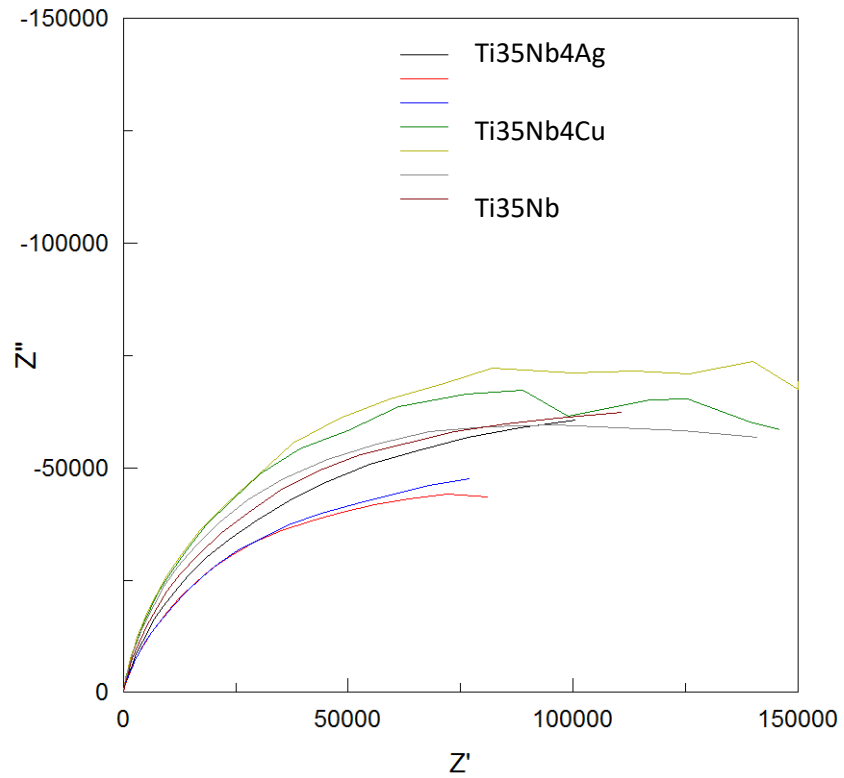
In the Nyquist diagrams shown in Figure 20 for copper-containing alloys and in Figure 22 for silver-containing alloys, the following can be seen :

First of all, in the case of Ti35NbXAg alloys, the lower the Ag content, the steeper the slope of the diagrams. On the other hand, in the case of Ti35NbXCu alloys, the slope is steepest for the alloy containing 4% copper, then the one containing 2, and finally the one containing 6. A higher slope means a higher resistance to electrochemical corrosion [12]. Moreover, figures 28, 29 and 30 that follow highlight these statements.



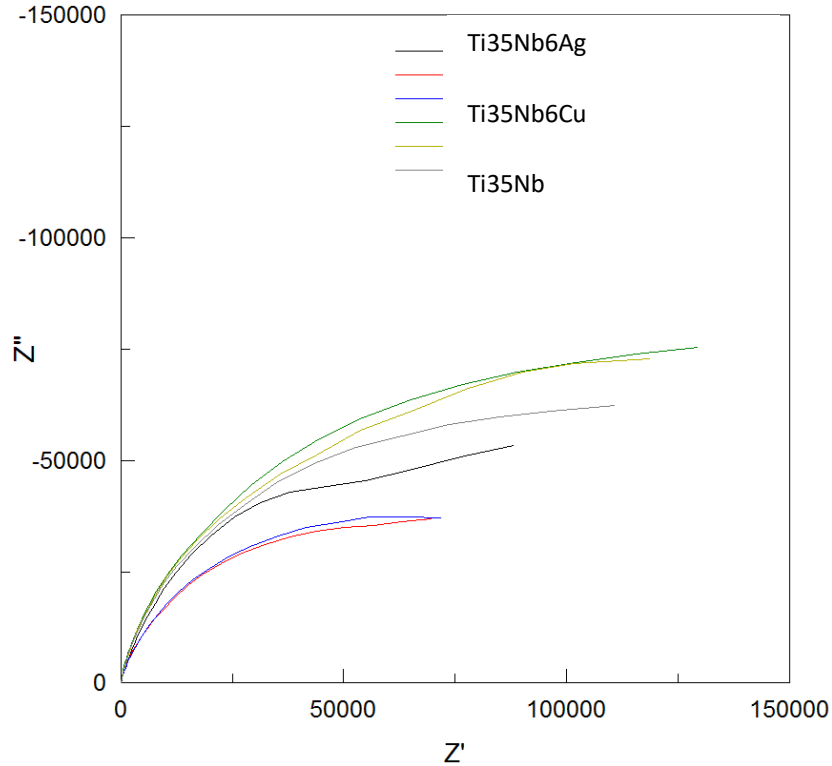
**Figure 28 :** Nyquist diagram comparing the studied alloys containing 2% copper or silver.





**Figure 29** : Nyquist diagram comparing the studied alloys containing 4% copper or silver.

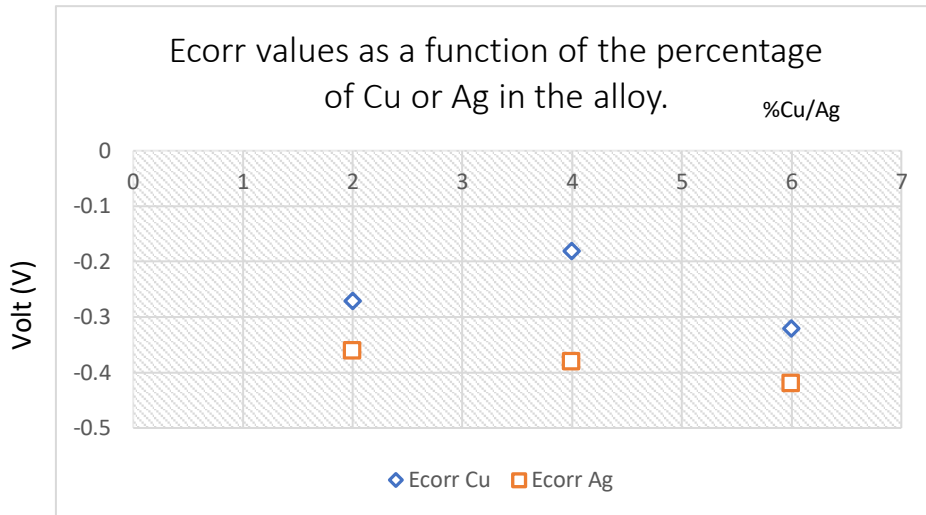
It can be seen that for alloys containing 4% of metal added to the Ti35Nb base, a change occurs; from now on, the slopes are greater for alloys containing copper than silver. This is still the case for a grade of 6% as shown in Figure 30.



**Figure 30 :** Nyquist diagram comparing the studied alloys containing 6% copper or silver.

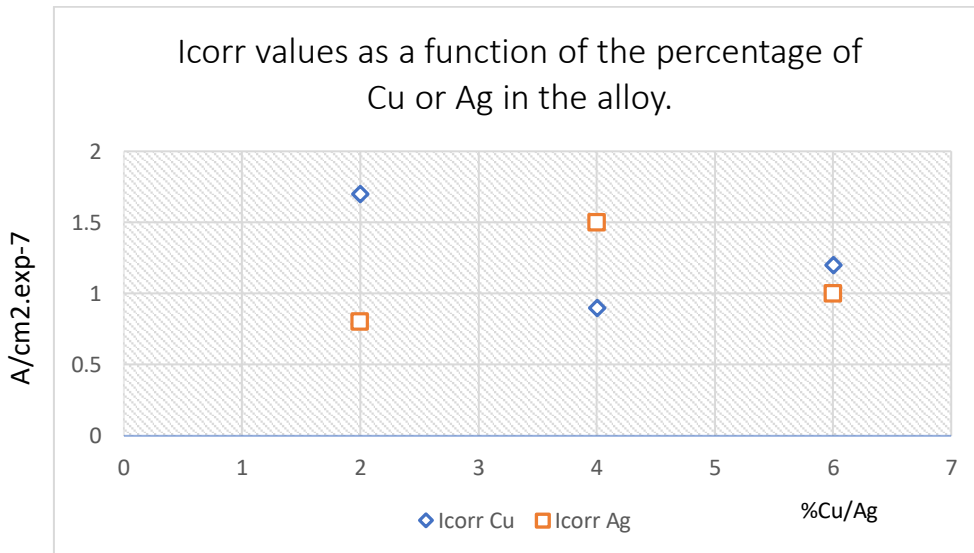
Moreover, it seems that for each experiment, the higher the copper content, the better the corrosion resistance, from this point of view, compared to the base alloy Ti35Nb.

Figure 31 shows the average  $E_{corr}$  values obtained for each alloy. It can be seen that the potential becomes more electronegative as the Ag content increases to get very close to the  $E_{corr}$  value of the base alloy Ti35Nb which is -0.43 V. On the other hand, for alloys containing copper, Ti35Nb4Cu has the highest  $E_{corr}$  value. This indicates that the addition of Ag has a negative influence on the corrosion resistance of alloys, and the addition of Cu has a positive influence, because a lower electronegative potential indicates a higher nobility of the metal and thus a better corrosion resistance [12,15].



**Figure 31** : Ecorr values as a function of the percentage of Cu or Ag in the alloy.

The analysis of the corrosion current density shown in Figure 32 shows more disparate results. Indeed, a metal will have better corrosion resistance the lower the  $I_{corr}$  value. Here, the lowest value of  $I_{corr}$  is that of Ti35Nb2Ag, followed very closely by the Ti35Nb4Cu alloy. Nevertheless, for metals containing 6% copper or silver, the values are very similar. This confirms what was seen in the Nyquist diagrams, namely a reversal of trend as soon as 4% copper is added to the Ti35Nb base, which improves corrosion resistance.



**Figure 32** : Icorr values as a function of the percentage of Cu or Ag in the alloy.

## **CHAPTER 6. CONCLUSIONS**

From the results and their analysis, we can deduce which alloys are most resistant to corrosion. On the one hand, it is interesting to remember that the choice of copper and silver is not insignificant, but was made because they are two metals that do not cause any undesirable effects to the body and are not toxic to it.

However, the results obtained and explained in the previous chapter tend to show that the addition of copper is beneficial in making the alloy more resistant to corrosion. This is also due to the fact that at the microstructural level, since the beta phase is predominant in the samples studied, copper will mix better with Titanium and Niobium, which will cause less porosity in the alloys contrary to silver which, added to the Ti35Nb base, will create many pores and therefore a greater ease for corrosion to form by attacking the metal through these same pores. However, alloys containing Silver are still those with the best mechanical properties, as discussed in the introduction.

The difference in the results on the study of the same sample may be due to the following factors; first of all, the aforementioned porosity plays an important role, especially when the samples, after each experiment, and before it is repeated, are polished and cleaned, which means that the study surface is no longer strictly identical. Moreover, since the experiments were carried out over several weeks, the artificial saliva used did not always have exactly the same PH, even if its composition remained approximately the same, since each element introduced was weighed vigorously and very precisely.

## CHAPTER 7. BIBLIOGRAPHY

- [1] Li Y, Yang C, Zhao H, Qu S, Li X, Li Y. New Developments of Ti-Based Alloys for Biomedical Applications. *Materials (Basel)*. 2014 Mar 4;7(3):1709-1800. doi: 10.3390/ma7031709. PMID: 28788539; PMCID: PMC5453259.
- [2] K. Swierkot, P. Lottholz, L. Flores-de-jacoby, & R. Mengel, "Success, and Survival of Implants", *Journal of Periodontology*, pp. 1213–1225, 2012.
- [3] V. Amigó. "Influencia de las adiciones de Fe en las aleaciones de Ti-Nb-Ta obtenidas mediante tecnología de polvos, para aplicaciones biomédicas". Ph.D, Universidad Politécnica de Valencia, Valencia, España, 2017.
- [4] J. Liu, X. Zhang, H. Wang, F. Li, M. Li, K. Yang & E. Zhang. "The antibacterial properties and biocompatibility of a Ti–Cu sintered alloy for biomedical application". *Biomed. Materials*, vol. 9, nº2.
- [5] V. Noronha, A. Paula, G. Durán, A. Galembeck, K. Cogo-Müller, M. Franz-Montan & N. Durán. "Silver nanoparticles in dentistry". *Dental Materials*, vol. 33, pp. 1110–1126, 2017.
- [6] Alexandra Sourdot. La Corrosion du titane en milieu buccal. *Sciences du Vivant [q-bio]*. 2007. hal-01733037
- [7] Société Francophone des Biomatériaux Dentaires (SFBD) G. GREGOIRE, B. GROSGOGEAT, P. MILLET ET PH. ROCHE
- [8] Electrochemical Corrosion and Impedance Studies of Porous Ti–xNb–Ag Alloy in Physiological Solution M. J Shivaram<sup>1</sup>, Shashi Bhushan Arya<sup>1</sup>, Jagannath Nayak<sup>1</sup>, Bharat B. Panigraha
- [9] DESARROLLO DE ALEACIONES TITANIO-NIOBIO-COBRE Y TITANIONIOBIO-PLATA MEDIANTE PULVIMETALURGIA PARA SU APLICACIÓN COMO BIOMATERIALES ANTIBACTERIANOS, DANIEL PADILLA ALFARO, 2018-2019
- [10] *Traité des Matériaux. Vol 12: Corrosion et chimie de surfaces des métaux.* Von D. Landolt. Presses Polytechniques et Universitaires Romandes. Lausanne 1993. Preis: SF 118,–
- [11] Jennifer Dupuis. Investigation d'alliages à base de titane de types béta-métastables pour applications marines: cas particulier d'un winch innovant. *Matériaux*. INSA de Rennes, 2014
- [12] Dieter Landolt, *CORROSION AND SURFACE CHEMISTRY OF METALS* 2007
- [13] A. Karayan et al. "Corrosion behavior of Ti – Ta – Nb alloys in simulated physiological media". *Materials Letters*, vol. 62(12–13), pp. 1843– 1845, 2008.

[14] J. Navarro Laboulais, A. Amigó Mata, V. Amigó Borrás, A. Igual Muñoz. “Electrochemical characterization and passivation behaviour of new betatitanium alloys (Ti<sub>35</sub>Nb<sub>10</sub>Ta-xFe)”. *Electrochimica Acta*, vol. 227, pp. 410–418, 2017.

[15] R. Chelariu et al. “Metastable beta Ti-Nb-Mo alloys with improved corrosion resistance in saline solution”. *Electrochimica Acta*, vol.137, pp. 280–289, 20

# **DOCUMENT 2**

## **BUDGET**

# CHAPTER 1 : BUDGET

## 1.1. Coste de personal

CUADRO DE PRECIOS MANO DE OBRA		
Nº	Concepto	Precio
1	Catedrático de Universidad (Director)	51,8€/h
2	Titular de Escuela Universitario (Ingeniero)	31,0€/h
3	Ayudante doctor (Técnico)	23,4€/h

Tabla 1. Cuadro de precios de personal.

## 1.2. Presupuesto descompuesto por fases.

CONCEPTO	COSTE/UD	CANTIDAD	COSTE TOTAL
<b>Discusión de la planificación del proyecto</b>			
<i>Personal</i>			
Catedrático/a de Universidad (Director)	51,80 €/h	10,00 h	518,00 €
Titular de Universidad (Ingeniero)	31,00 €/h	10,00 h	310,00 €
<b>SUBTOTAL 1</b>			<b>828,00 €</b>
<b>Revisión bibliográfica</b>			
<i>Personal</i>			
Titular de Universidad (Ingeniero)	31,00 €/h	30,00 h	930,00 €
<b>SUBTOTAL 2</b>			<b>930,00 €</b>
<b>Formación (Software, Maquinaria, etc.)</b>			
<i>Personal</i>			
Titular de Universidad (Ingeniero)	31,00 €/h	5,00 h	155,00 €
Ayudante Doctor (Técnico)	23,40 €/h	5,00 h	117,00 €
<b>SUBTOTAL 3</b>			<b>272,00 €</b>
<b>TOTAL</b>			<b>2.030,00 €</b>

Tabla 4. Presupuesto para la planificación del proyecto, revisión bibliográfica y formación necesaria.



### 1.3. Presupuesto de saliva artificial.

<i>Materiales, Utillajes, Equipo</i>			
Saliva Artificial	6,00 €/L	2,00 L	12,00 €
Laca de uñas	30,00 €/L	0,03 L	0,90 €
Calibre R5 Components	0,03 €/h	0,75 h	0,02 €
Balanza Kern PFB 300	0,06 €/h	1,50 h	0,09 €
<i>Maquinaria</i>			
Estufa Selecta modelo 2000207	0,16 €/h	730,00 h	116,80 €
<i>Personal</i>			
Ayudante doctor (Técnico)	23,40 €/h	4,00 h	93,60 €
<b>SUBTOTAL</b>			<b>223,41 €</b>

Tabla 3 : Preparación de saliva artificial.

### 1.4 Presupuesto para estudios electroquímicos.

<i>Materiales, Utillajes, Equipo</i>			
Electrodo Ag/AgCl Metrohm AUTOLAB	0,19 €/h	28,00 h	5,43 €
Contraelectrodo Platino Radiometer Analytica	0,14 €/h	28,00 h	3,82 €
Termopar	0,09 €/h	28,00 h	2,55 €
Lámpara halógena	0,02 €/h	28,00 h	0,42 €
Electrolito NaCl 1M	5,00 €/L	3,00 L	15,00 €
Disolución Acetona-etanol	10,00 €/L	0,20 L	2,00 €
<i>Maquinaria</i>			
Potenciostato Metrohm AUTOLAB modelo PGSTAT204	1,70 €/h	28,00 h	47,66 €
<i>Personal</i>			
Ayudante doctor (Técnico)	23,40 €/h	28,00 h	655,20 €
<b>SUBTOTAL</b>			<b>732,08 €</b>
<b>TOTAL</b>			<b>949,95 €</b>

Tabla 4: Presupuesto para estudios electroquímicos

## 1.5 Presupuesto para la redacción del proyecto.

CONCEPTO	COSTE/UD	CANTIDAD	COSTE TOTAL
<b>Redacción de la memoria</b>			
<i>Personal</i>			
Titular de Universidad (Ingeniero)	31,00 €/h	252,00 h	7.812,00 €
SUBTOTAL			7.812,00 €
<b>Revisión de la memoria</b>			
<i>Personal</i>			
Catedrático/a de Universidad (Director)	51,80 €/h	20,00 h	1.036,00 €
Titular de Universidad (Ingeniero)	31,00 €/h	20,00 h	620,00 €
SUBTOTAL			1.656,00 €
<b>TOTAL</b>			<b>9.468,00 €</b>

Tabla 5. Presupuesto para la redacción del proyecto

## 1.5 Subtotales totales y suma final

<b>Subtotales</b>	
<b>totales</b>	12 668,36 €
<b>L.V.A 21%</b>	2 660,35 €
<b>Suma final</b>	<b>15 328,72 €</b>